REPUBLIC OF ZAMBIA
Ministry of Energy and
Water Development

FEDERAL REPUBLIC OF GERMANY
Federal Institute for
Geosciences
and Natural Resources

Development of a Groundwater Information & Management Program for the Lusaka Groundwater Systems

REPORT NO. 3

Karstification, Tectonics and Land Use in the Lusaka Region

Kai Hahne & Beauty Shamboko-Mbale

Lusaka, September 2010

REPORT N° 3

Karstification, Tectonics and Land Use in the Lusaka Region

Author	Dr. Kai Hahne (BGR) Beauty Shamboko-Mbale (DWA)
Commissioned by	Federal Ministry for Economic Cooperation and Development (BMZ: Bundesministerium für wirtschaftliche Zusammenarbeit und Entwicklung)
Project Number	BMZ PN 2008.2125.6
BGR	B4.4-10699/10
Implementing Agencies	Ministry of Energy and Water Development, Department of Water Affairs, Lusaka Federal Institute for Geosciences and Natural Resources (BGR: Bundesanstalt für Geowissenschaften und Rohstoffe, Hannover)
Pages	76
Place and date of issuance	Hannover, September 2010

Table of Contents

Appendix

- **TABLE OF WAYPOINTS**
- **GENERALISED LAND USE MAP, SCALE 1:200,000**
- **ARCVIEW-PROJECT DVD**

Abbreviations

BGR	Bundesanstalt für Geowissenschaften und Rohstoffe (Federal Institute for Geosciences and Natural Resources)
DEM	Digital Elevation Model
DWA	Department of Water Affairs
ETM	Enhanced Thematic Mapper
GIS	Geographic Information System
GPS	Global Positioning System
m asl	Metres above sea level
MSZ	Mwembeshi Shear Zone
Pmax	maximum principal stress
Pmin	minimum principal stress
RGB	Red Green Blue (colour bands combination)
SPOT	Satellite Pour l´Obsevation de la Terre
SRTM	Shuttle Radar Topography Mission
WP	Way Point (measured by GPS)

List of figures

1 Scope of Work

Within the bilateral project “Development of a Groundwater Information & Management Program” between BGR and the Department of Water Affairs (DWA), Ministry of Energy and Water Development, Zambia, one focus lies upon groundwater quality and its vulnerability to pollution.

Therefore a detailed knowledge of possible water flow paths within aquifers as well as the specific delineation of different land use is essential.

Existing maps are not sufficient to meet these requirements within the working area. For this reason, the scope of the assignment in the BGR-DWA program was to

- verify currently existing geological data in the field;
- delimit karst features, major fault- and fracture zones by various remote sensing methods and to verify them in the field;
- verify and describe karst dimensions in the field, which cannot be detected on remote sensing data due to soil- and vegetation cover;
- Verify land use information, which was drawn from remote sensing data before.

Field work was done from 04/06/2009 to 30/06/2009. Preliminary results have been presented and discussed with the BGR-DWA project team at the end of the mission.

2 Working Area

The working area comprises the coverage of the planned Hydrogeological Map of Zambia, Lusaka Province, at the scale of 1 : 100.000 with Zambia's capital Lusaka in the centre (figure 1). Its geographical corners are 27°51´E / 15°08´24"S in the NW and 28°45´E / 15°38´24"S in the SE.

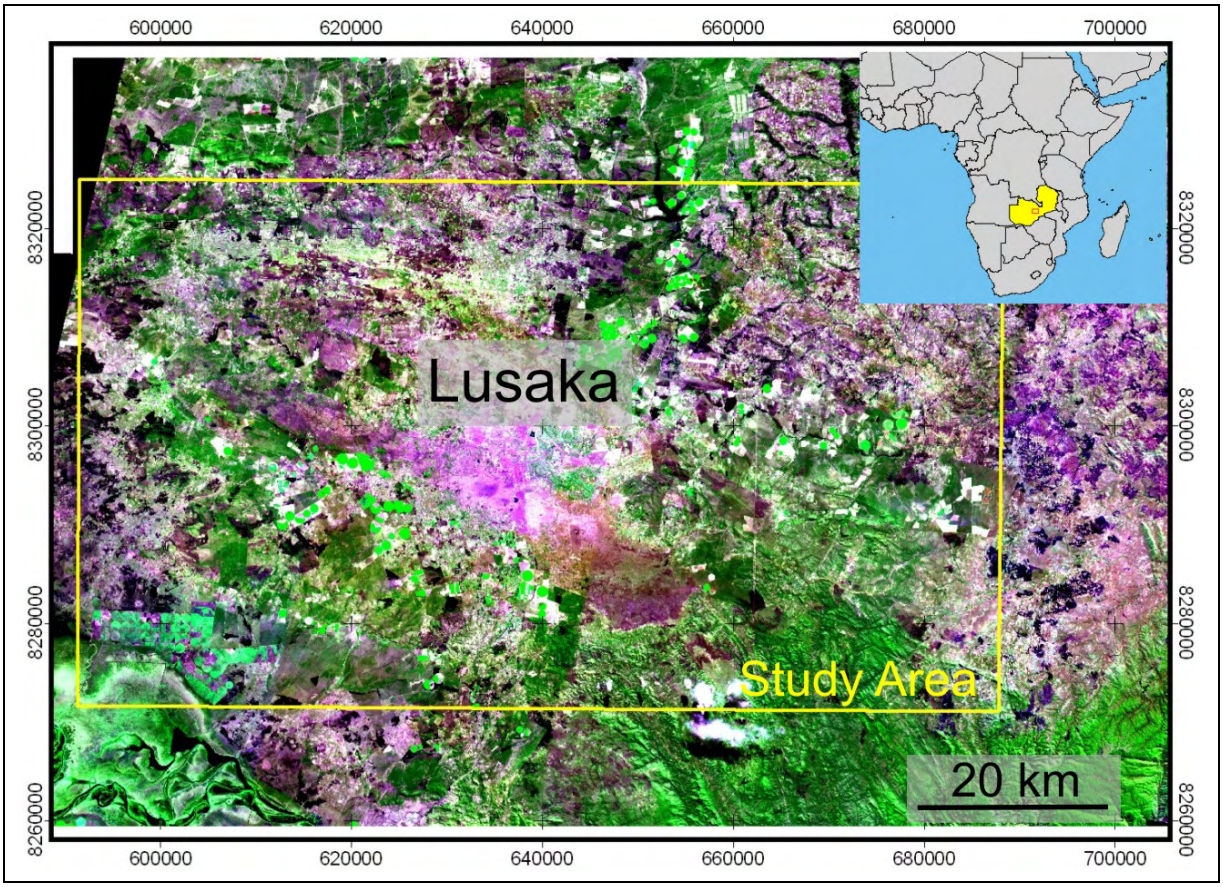

Figure 1: Location of the working area in Zambia marked by yellow frame. SPOT bands 1,2,3 (RGB)

The main part of the groundwater recharge area is situated on the Lusaka plateau, expanding from Mwembeshi in the NW to the Shantumbu area about 20 km to the SE of Lusaka. The highest point of the plateau is situated in the SE at 1377 m above sea level (asl). The lowest point is situated in the Kafue flats in the SW at 975 m asl (figure 2).

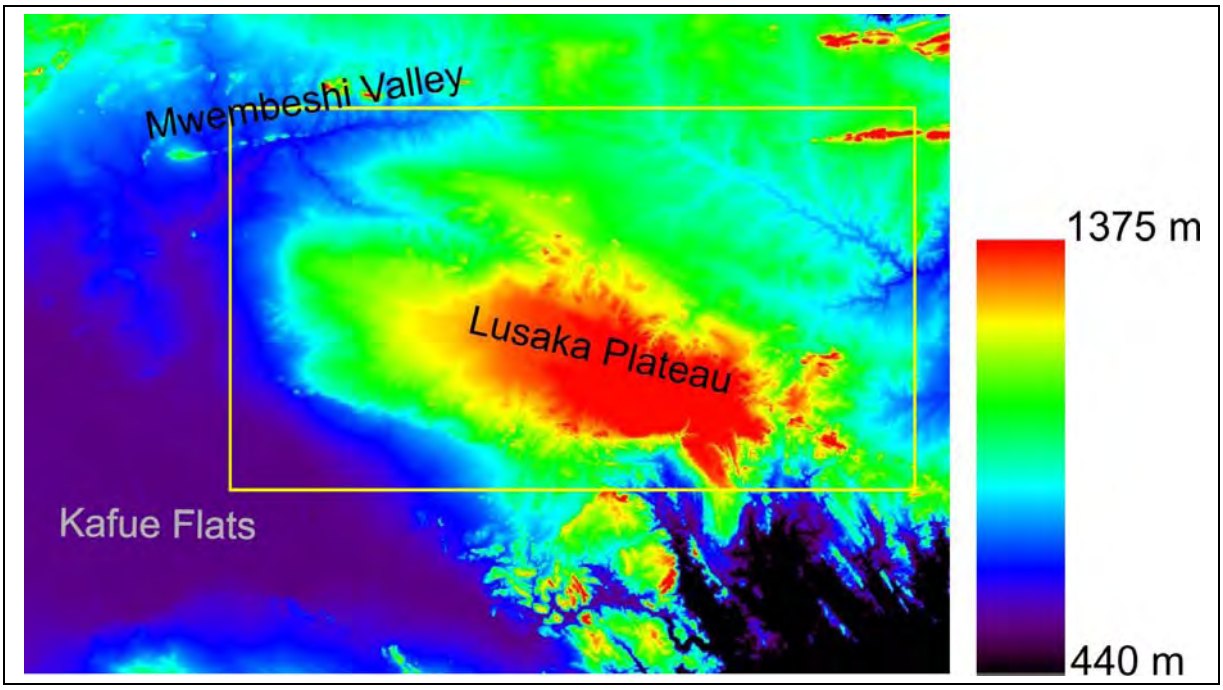

Figure 2: Location of the working area in Zambia in SRTM DEM with colour-coded altitudes

One focus of field work was the area NW of Lusaka, as no karst-related field data have been evaluated within this project so far. This area shows only very sparse outcrops and is covered with soil and thick scrubland.

3 Data

The following data were used within Arc View GIS (version 3.2) for further analysis and fault vectorization:

- Enhanced and geocoded satellite images:
    - Landsat TM acquired May, 13, 2002
    - SPOT acquired July, 11, 2008 (western part), August, 13, 2007 (north east), July, 14, 2007 (south east)
    - SRTM digital elevation model
    - Quickbird from Google Earth; various acquisition dates from 2004 and 2006
- Geocoded raster data:
    - Geological maps
        - Map Sheet 1527NE: Mwembeshi (Simpson 1962),
        - Map Sheet 1528NW: Lusaka (Simpson et al. 1963),
        - Map Sheet 1528NE: Chainama (Garrard 1968).
- Vector data:
    - Geological maps
        - Map Sheet 1527NE: Mwembeshi (Simpson 1962),
        - Map Sheet 1528NW: Lusaka (Simpson et al. 1963),
        - Map Sheet 1528NE: Chainama (Garrard 1968).
- Information from field work:
    - Dimensions of karst holes
    - Layer dip/strike
    - Additional geological and tectonical information
    - Information of land use (type of field crops etc.)
    - Field photos
    - Waypoints (WP) from GPS measurements.

Coordinates of all locations surveyed in the field were taken with GPS (Garmin 60 CSx, average accuracy of +/- 5 m). This information was afterwards entered into GIS tables.

The spatial reference system used as standard within the DWA is the Arc 1950 Zambia coordinate system. For this study, UTM 35 S, WGS 84 was used. Therefore data layers as “geology” had to be reprojected. Reprojection of shape and grid files was achieved by using ArcGIS.

The following layers have been created:

- Major lineaments
- Minor lineaments.
- Dip
- Karst
- A slightly simplified geological map (“Geology_wgs84_simpson_reduced”), combining the existing sheets.

Land use layers:

- Water
- Settlement
- Forest
- Agriculture
- Bare soil plinthic
- Bare soil plinthic 1
- Bare soil

The whole data is attached on DVD to this report as an ArcView-project. In figures, showing field photos, the location refers to a waypoint (WP) listed in the data tables in the appendix.

4 Tectonical setting

The main structural trend of the working area is NW-SE.

The Katanga series are affected by at least three phases of deformation (Barr, 1968, Matheson & Newman, 1966 in Nkhuwa, 1996):

1. Early large-scale F_1-recumbent folding with NW-SE-trending axes, overturned towards the SW. This phase is probably contemporaneous with D_1-thrusting, directed from SW to NE and has affected all rocks.
2. Open F_2-folds with axes also to the NW-SE, which have refolded the recumbent folds.
3. Open F_3-folds with axes to the NE-SW.

According to Paroda & Berhorst (2000) NE-directed thrusting was succeeded by backfolding and backthrusting, re-displacing the platform carbonates like Lusaka Dolomite southwards (figure 3).

Low-angle-overthrusting in the Lusaka area resulted in a tectonical thickening of the marbles (Nkhuwa, 1996). In the area of Lusaka South Local Forest, slicken sides with movement directions of the hanging rock towards 120° and 165° indicate this low-angle-overthrusting, possibly a backthrusting (figure 4).

All measured layer dipping coincided well with the measurements in the existing geological maps from Simpson et al. (1962, 1963).

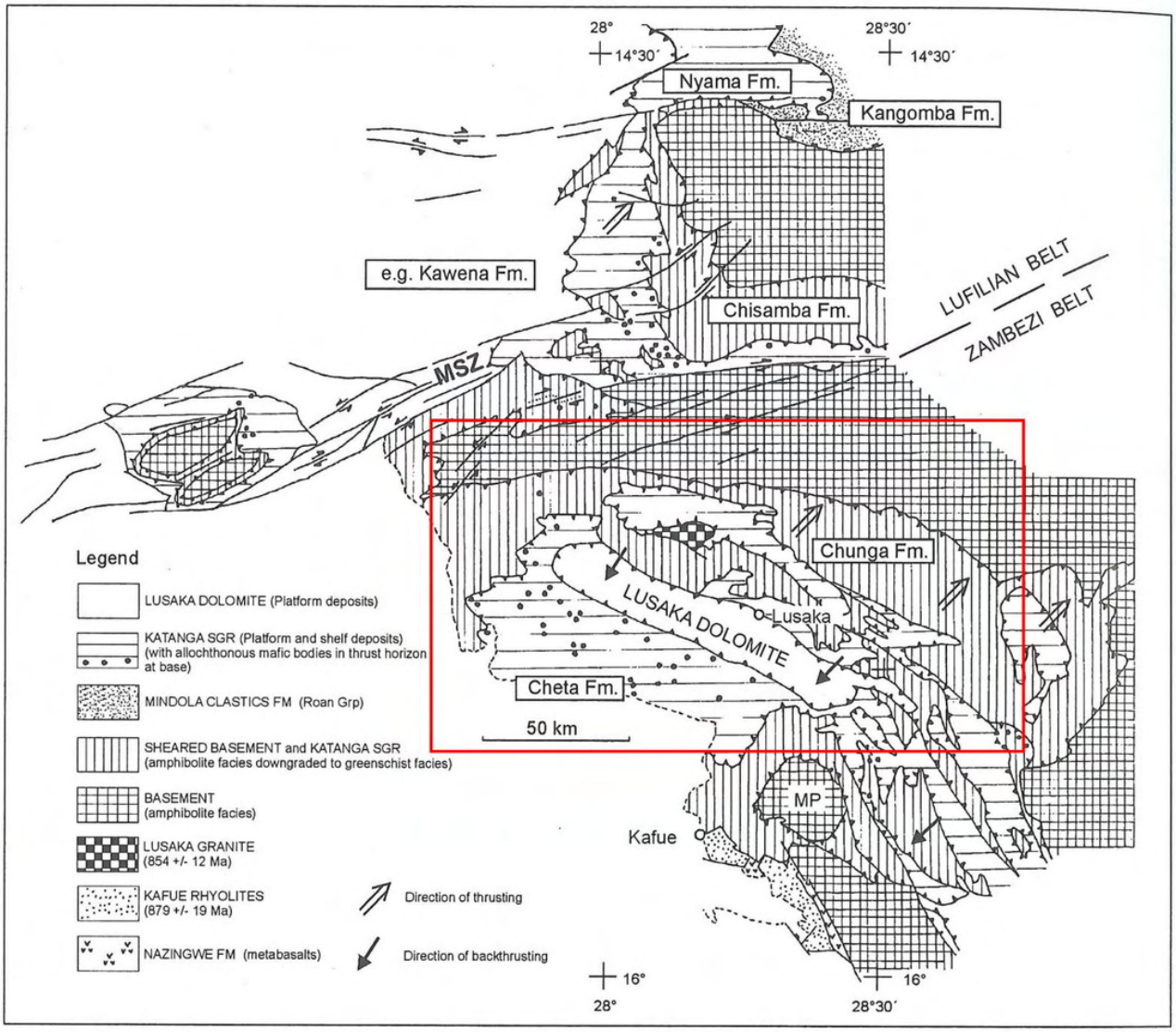

Tectonostratigraphical re-interpretation of parts of the Lufilian and Zambezi Belts adjoining the Mwembeshi Shear Zone (MSZ). Exposed are relics of a thrust wedge consisting of predominantly calcareous shelf and platform slope deposits that were thrust northeastwards onto a platform. Fragments of mafic rocks (●) were dragged along a thrust that climbed up the passive margin and involved the basement at the platform edge. In the northern Zambezi Belt, thrusting was succeeded by backfolding and backthrusting, re-displacing platform carbonates (e.g. Lusaka Dolomite) southwestwards. The Lusaka Granite is intrusive into basement (Chunga Formation) and tectonically overlain by Katanga Supergroup deposits (Cheta Formation). MP: Mpande Dome.

Figure 3: Tectonostratigraphical interpretation of Lufilian and Zambezi Belts after Paroda & Berhorst (2000). Red rectangle marks working area.

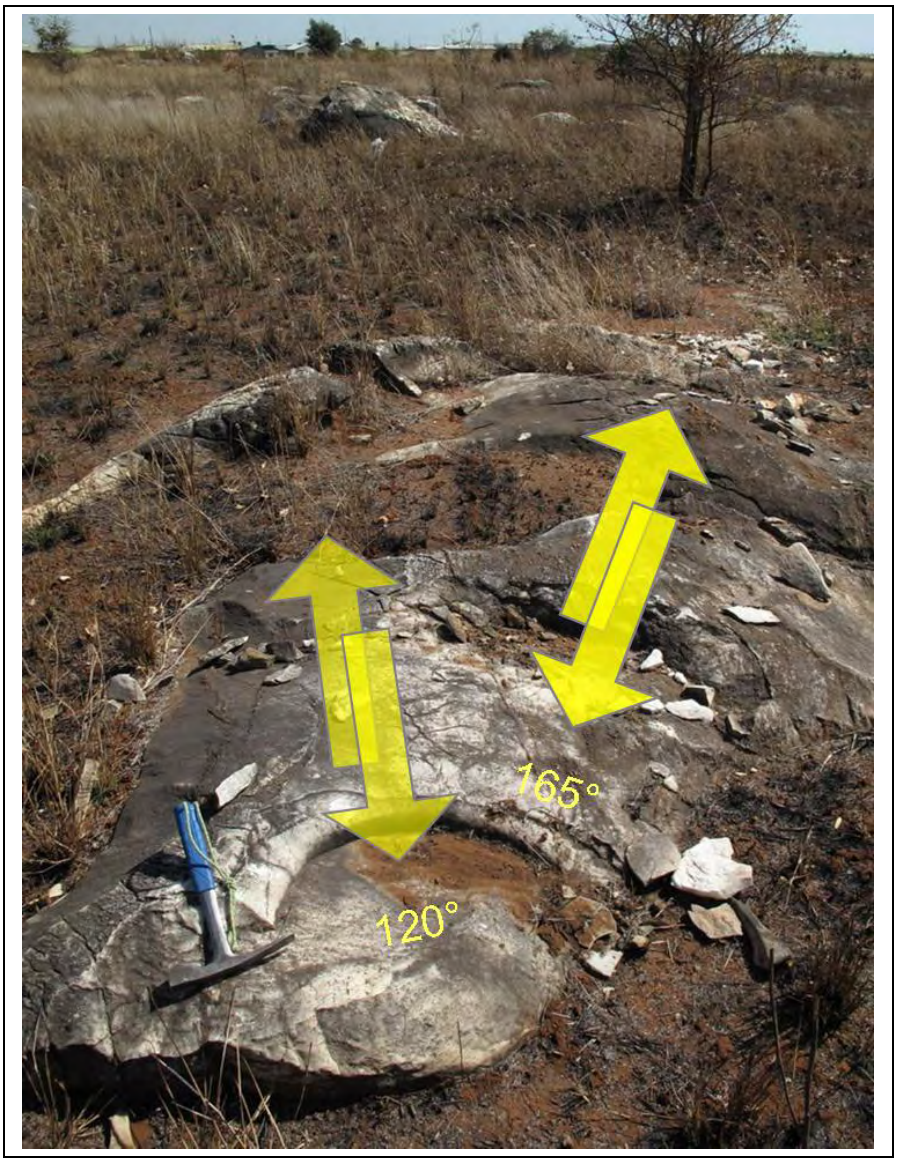

Figure 4: Low-angle-overthrusting with movement directions of the hanging rock towards 120° and 165° in the area of Lusaka South Local Forest, indicated by lunulate slicken sides. Waypoint (WP) 029.

4.1 Joints

According to Nkhuwa (1996), three major joint directions with distinct sets of orientation exist:

1. Steep dipping (80° - 90° towards the NW and SE) cross joints formed perpendicular to main fold axes, with strike directions between 030° to 060°.
2. Longitudinal joints parallel to the fold trends (strike 110° – 140°, dip 30 – 45° towards the SW).
3. Diagonal joints striking between 150° – 180° and a minor conjugate set striking between 060° and 080°, dipping 65° to 90° to the east and south.

This observation can be supported concerning strike directions, but must be completed, concerning the dip direction of longitudinal joints, as cleavage planes also dip steeply (75° to 80°) towards the NE (036° to 046°, figure 5).

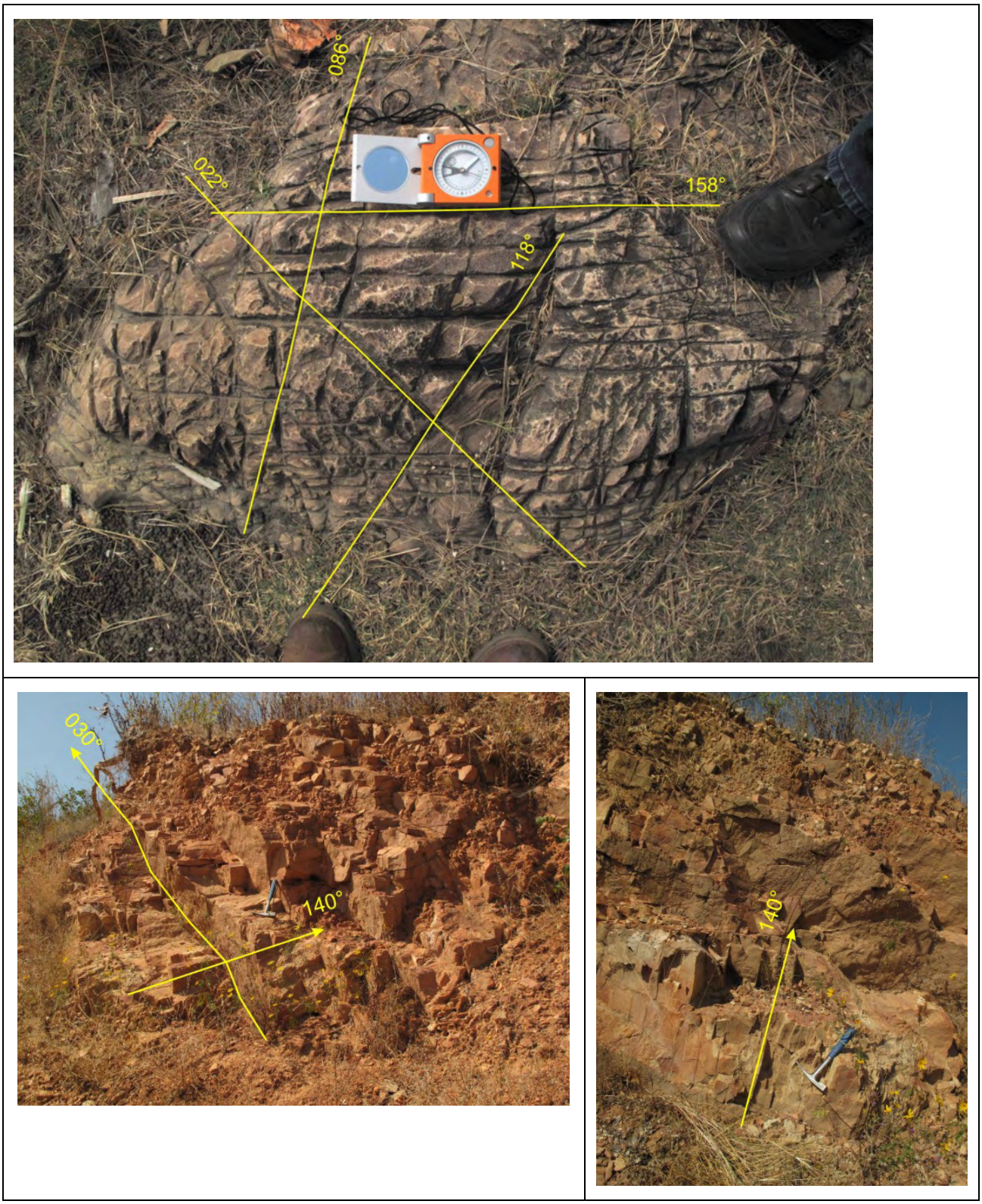

Figure 5 Above: steep joints in Lusaka Dolomite striking approx. parallel to fold trend (118°), diagonal (158°, 086°) and approx. perpendicular to main fold axes (022°) WP 016. Below: steep dipping cross- and longitudinal joints in a schist of the Cheta Formation with strike directions perpendicular (030°) and parallel (140°) to the main fold trend. Cleavage planes strike and dip towards 130-150/70-85 and 036-046/75-80 (WP 069).

4.2 Faults

Directions of maximum principal stress can be derived from satellite imagery, regarding the x-shaped stress indicators, which are found in the vicinity of the north-eastern part of the Mwembeshi Valley. The acute angle between conjugate faults is bisected by the maximum principal stress direction (Pmax). Direction of Pmin corresponds to the opening directions of Mid Zambezi- and Luangwa Rifts (figure 6).

In the working area three main trends/types of faults occur:

1. Strike direction NW – SE (approx. 120°), parallel to the main structural trend,
2. A further NW – SE direction (140°)
3. A probably conjugate NE – SW direction (035°, 045°).

   To a minor extent also a NE – SW trend (080°) paralleling the “Mwembeshi shear zone (MSZ) direction” is present (figures 7 and 8).

The Mwembeshi shear zone (MSZ) is considered as a pre-existing reactivated zone of weakness within the lithosphere, separating the Zambezi Belt from the Lufilian Belt in the north (Paroda & Berhorst, 2000, figure 3). It forms a brittle/ductile transform shear belt, up to 8 kilometres wide with predominantly left-lateral displacements (Nkhuwa 1996).

The northwestern part of the Mwembeshi valley inside the working area represents a branch of the MSZ (figure 6). Adjacent to this branch, fault directions described before (types 2. and 3.) occur. They often form local and regional streams (e.g. the Chunga River turns from a parallel fault of type 1 into a NW-trending fault of type 2. Mwembeshi River turns from a NE-trending fault parallel to MSZ into a NW-trending fault of type 2. to the W outside the working area). These faults occur with left-lateral, as well as right-lateral displacements (figure 9).

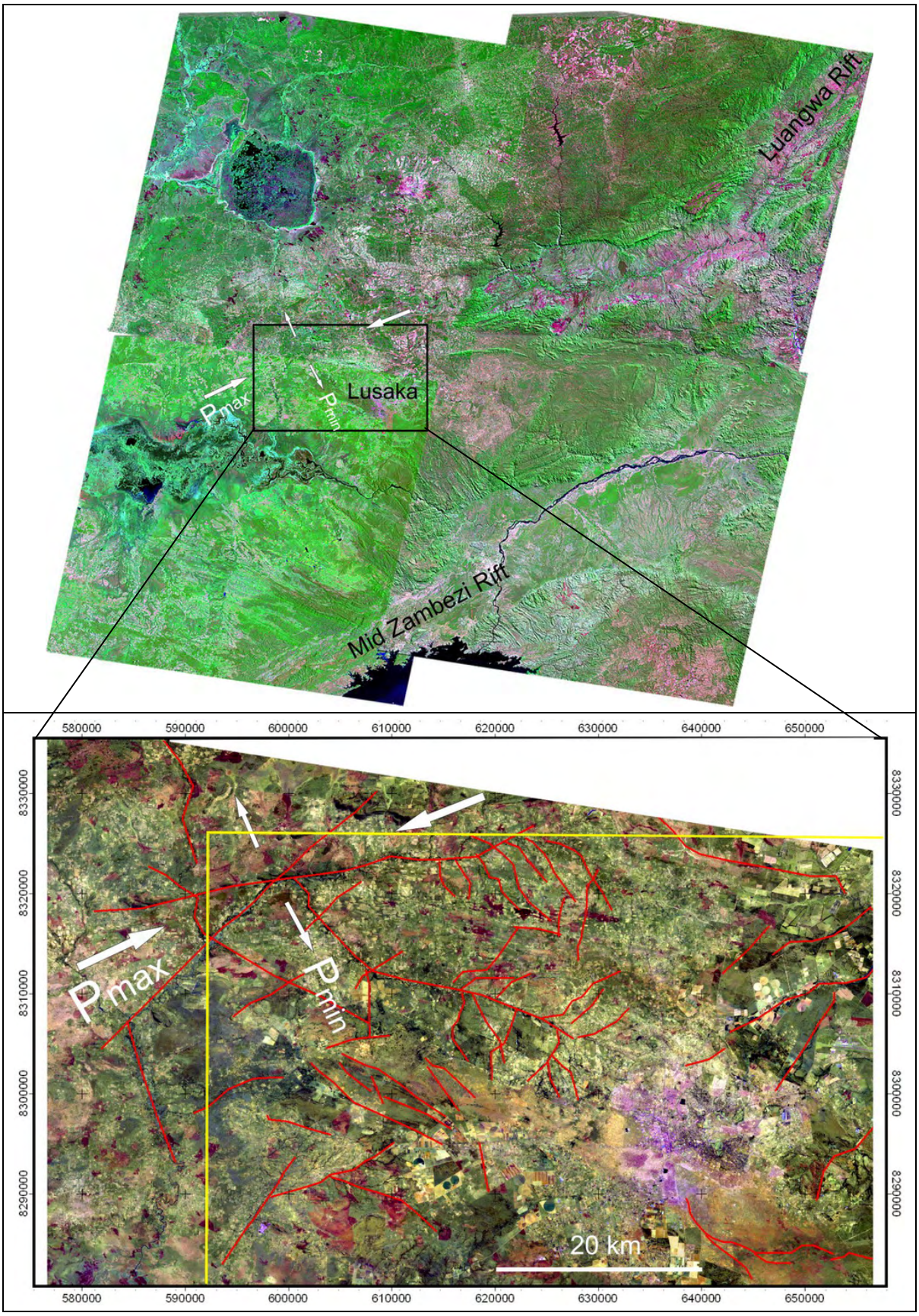

Figure 6: Above: Overview of the Lusaka area between Mid Zambezi- and Luangwa Rifts. Mosaic of 4 ETM scenes, bands 7,4,2 (RGB). Below: Close up view of examples of major faults and stress indicator along a fault in Mwembeshi valley. Effective Pmin direction coincides with the opening direction of the rifts. ETM bands 7,5,2 (RGB).

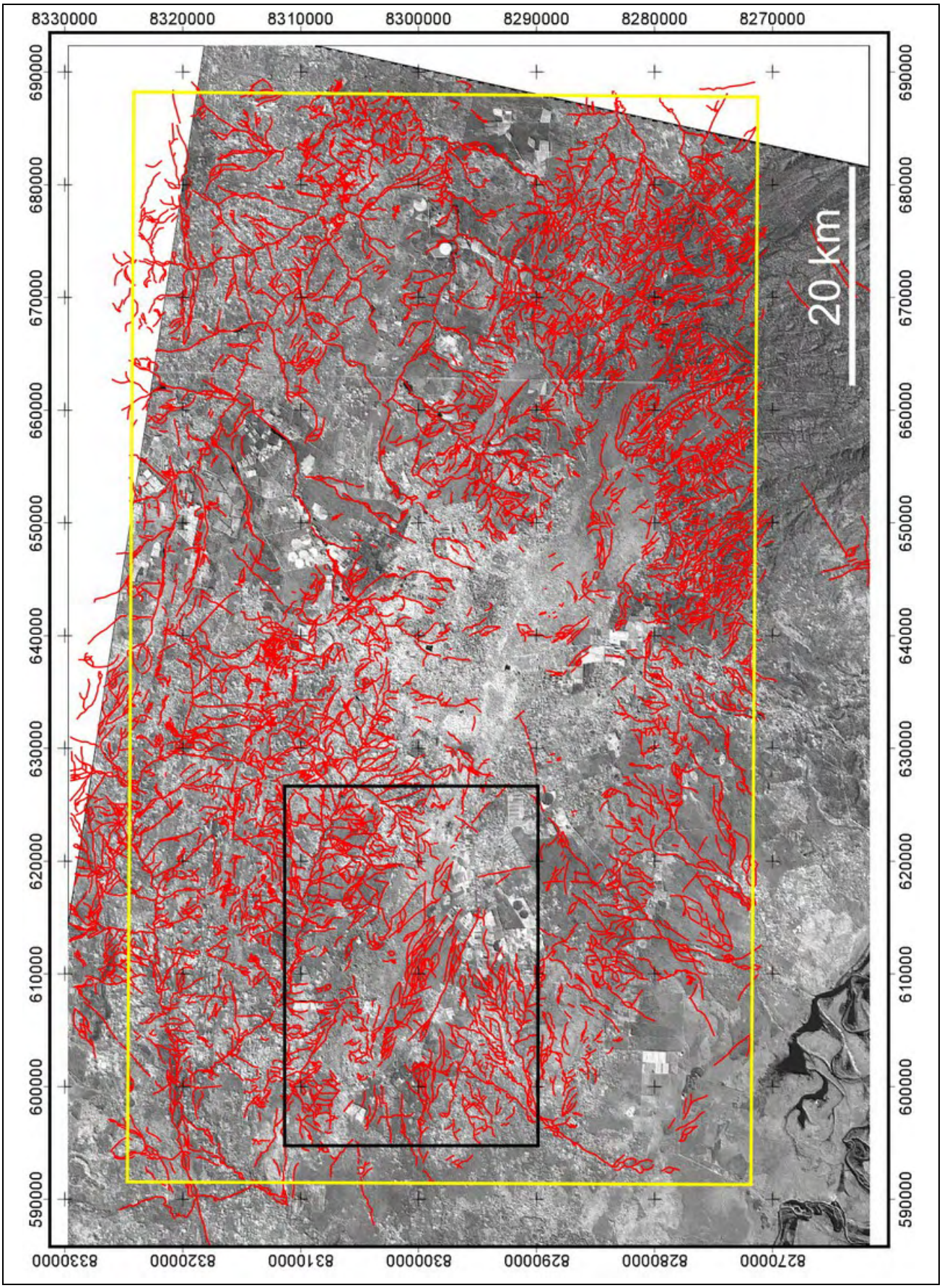

Figure 7: Examples for minor faults derived from satellite images projected into Landsat ETM band 5. Black rectangle marks area of shear lenses shown in figure 10.

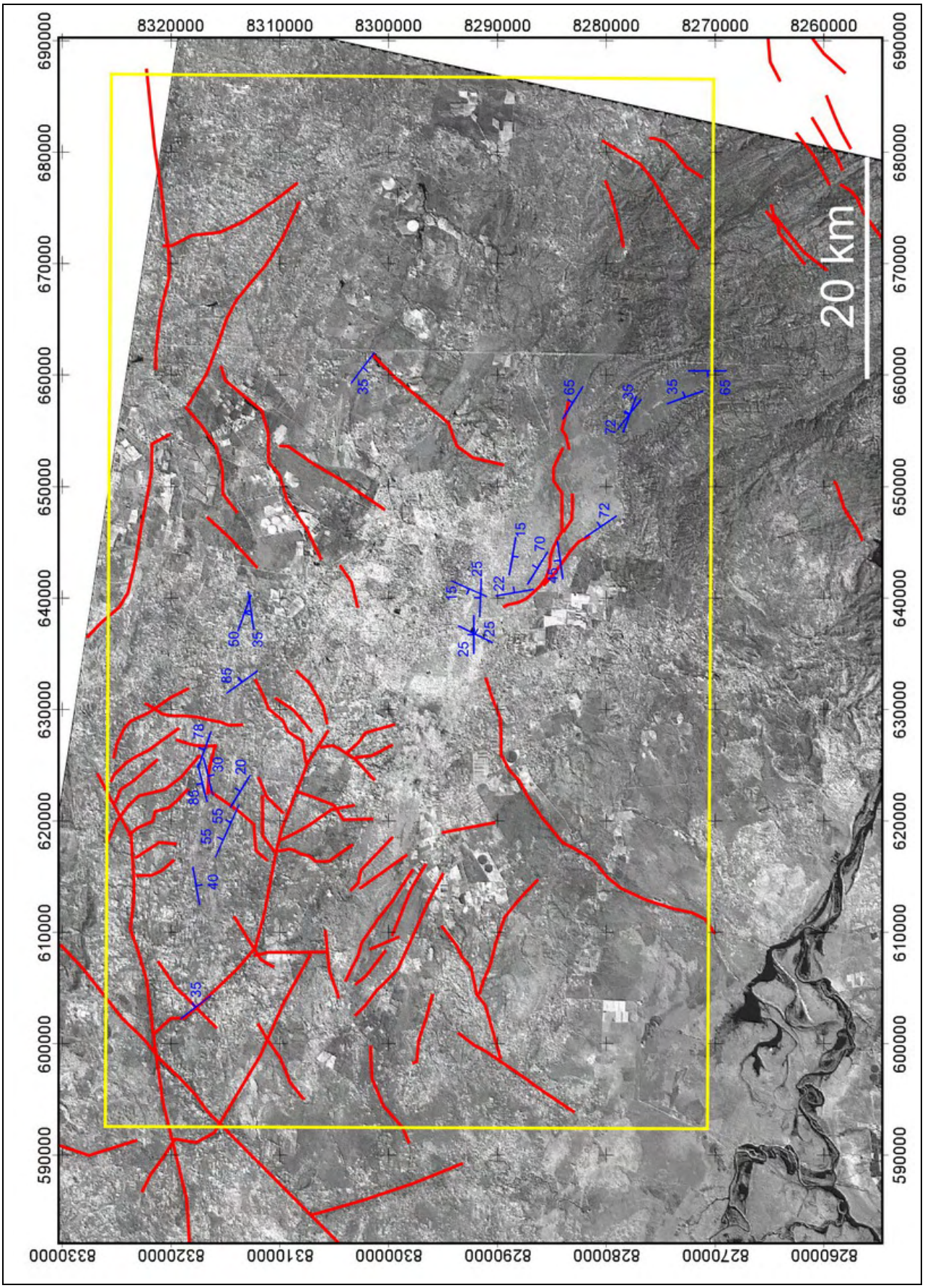

Figure 8: Examples for major faults derived from satellite images projected into Landsat ETM band 5. Layer dipping with dip angles shown in blue symbols.

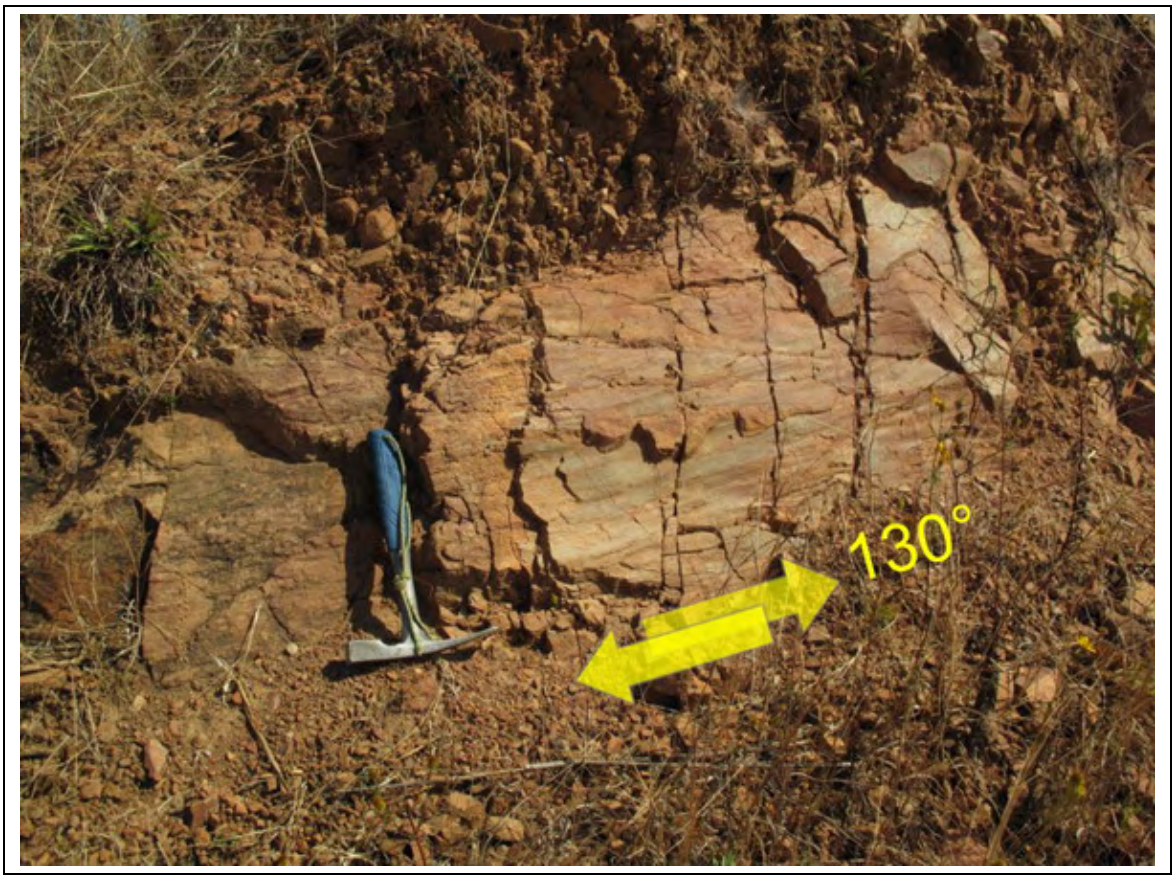

Figure 9: Fault plane in Cheta Formation striking 130° SE with slicken sides indicating a right-lateral movement. Vicinity of Momba School (WP 069).

In satellite images to the West and NW of Lusaka – by influence of the MSZ – almost any fault of all three types shows shear lenses with a fractal pattern. E.g. lenses of 17 km length to a few metres length can be observed (figure 10).

To the SE, increasing influence of the Zambezi-rift can be observed by NE-striking normal faulting and absence of shear lenses (figure 11).

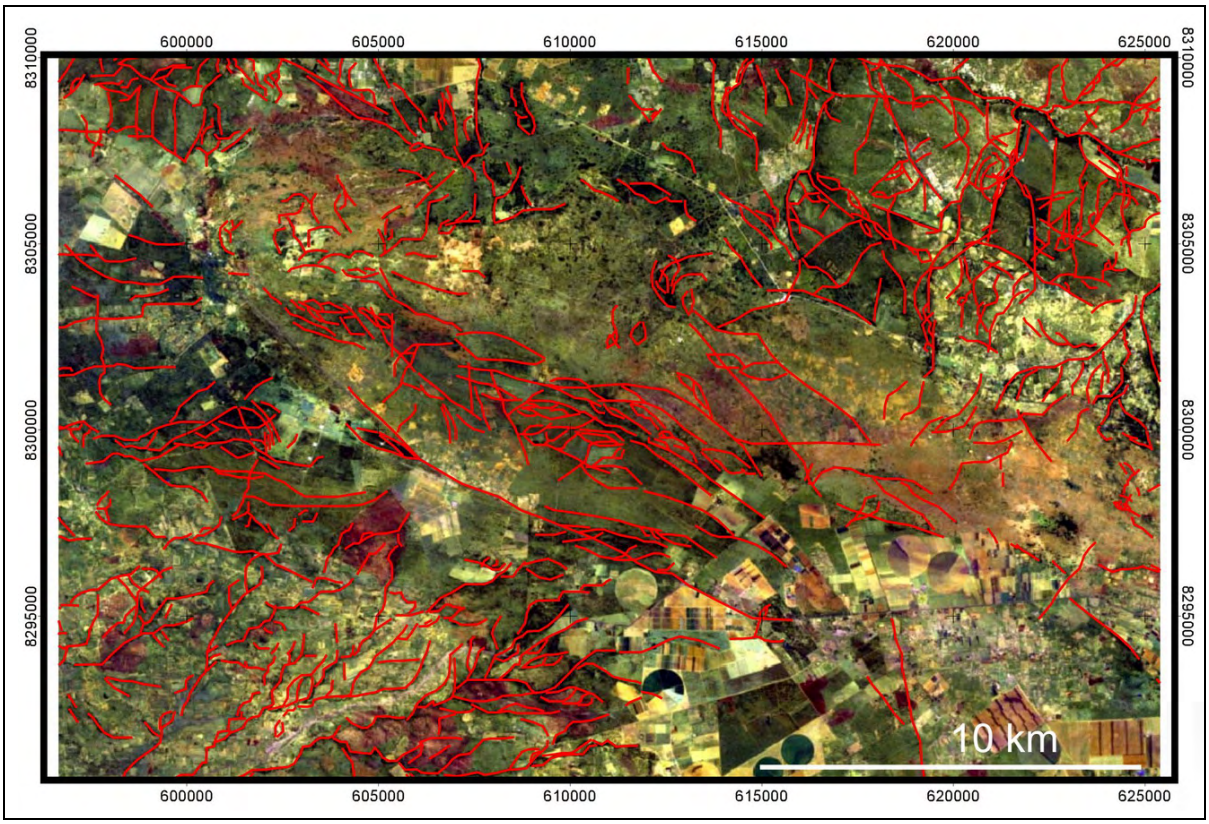

Figure 10: A fractal pattern of shear lenses bordered by faults (centre, red lines). An example from an area west of Lusaka within the influence of MSZ. Scale of the shear lenses ranges from 17 km to a few metres length. Faults defining shear lenses are commonly only visible by a change in colour contrasting with the surrounding area, unlike those faults that are enhanced by a pattern of streams and rivers. ETM bands 7,5,2 (RGB). Position within the working area is marked in figure 7 by black rectangle.

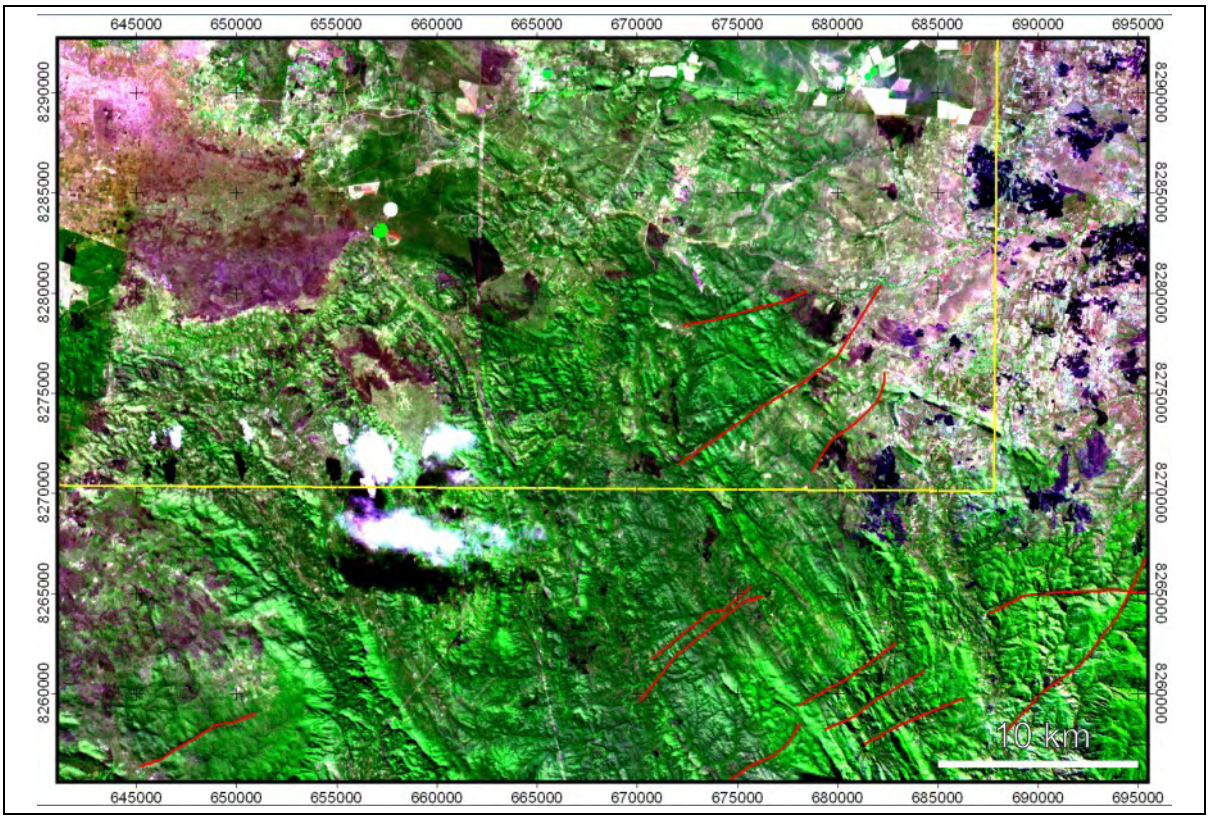

Figure 11: Increasing influence of the Zambezi Rift visible by normal faulting. Examples highlighted by red lines. SPOT bands 1,2,3 (RGB).

Examples of deep approx. vertical faulting can be found along a line of talc quarries within the Lusaka Dolomite Formation SE of the city. Talc deposits ($Mg_3Si_4O_{10}(OH)_2$) result from the transformation of existing rocks under the effect of hydro-thermal fluids carrying one or several of the components (MgO, SiO_2, CO_2), needed to form the mineral. Tectonics play a major role in the genesis of a talc deposits (figure 12, above). Further hints for former hydrothermal activity can be found in direct vicinity along-strike of the quarries in an occurrence of tall calcite crystals (figure 12, below).

Figure 12 Above: quarry of a talc deposit gives evidence for former hydrothermal activity within deep faults. Inset shows soft material of talc or “soapstone” respectively (WP 030). Below: tall calcite crystals in direct vicinity of talc deposit formed within a hydrothermal fault (WP 032).

5 Geology

The geological units of the working area are composed of Late Precambrian clastic meta-sediments and carbonate rocks, which were deposited before the pan African orogenesis and multiphase-deformed and overthrusted within the Zambezi Belt during the pan African orogenesis. They unconformably overlie an Early to Late Precambrian crystalline basement (Nkhuwa, 1996). Partially they are intruded by granites and basic bodies (Simpson, 1962, Simpson et al. 1963).

The rocks are part of the “Zambezi supracrustal sequence” (Hanson et al. 1994).

According to Simpson et al. (1963) the metasedimentary rock cover, belonging to the Katanga system, can be divided into three formations:

1. Chunga Formation (schist and quartzites),
2. Cheta Formation (schist and carbonates) and
3. Lusaka Dolomite Formation (carbonates).

Calcareous units of all formations show features of karstification.

Figure 13 shows an overview of the stratigraphical classification of the Zambezi supracrustal sequence according to various authors (Bäumle & Kang’omba, 2009).

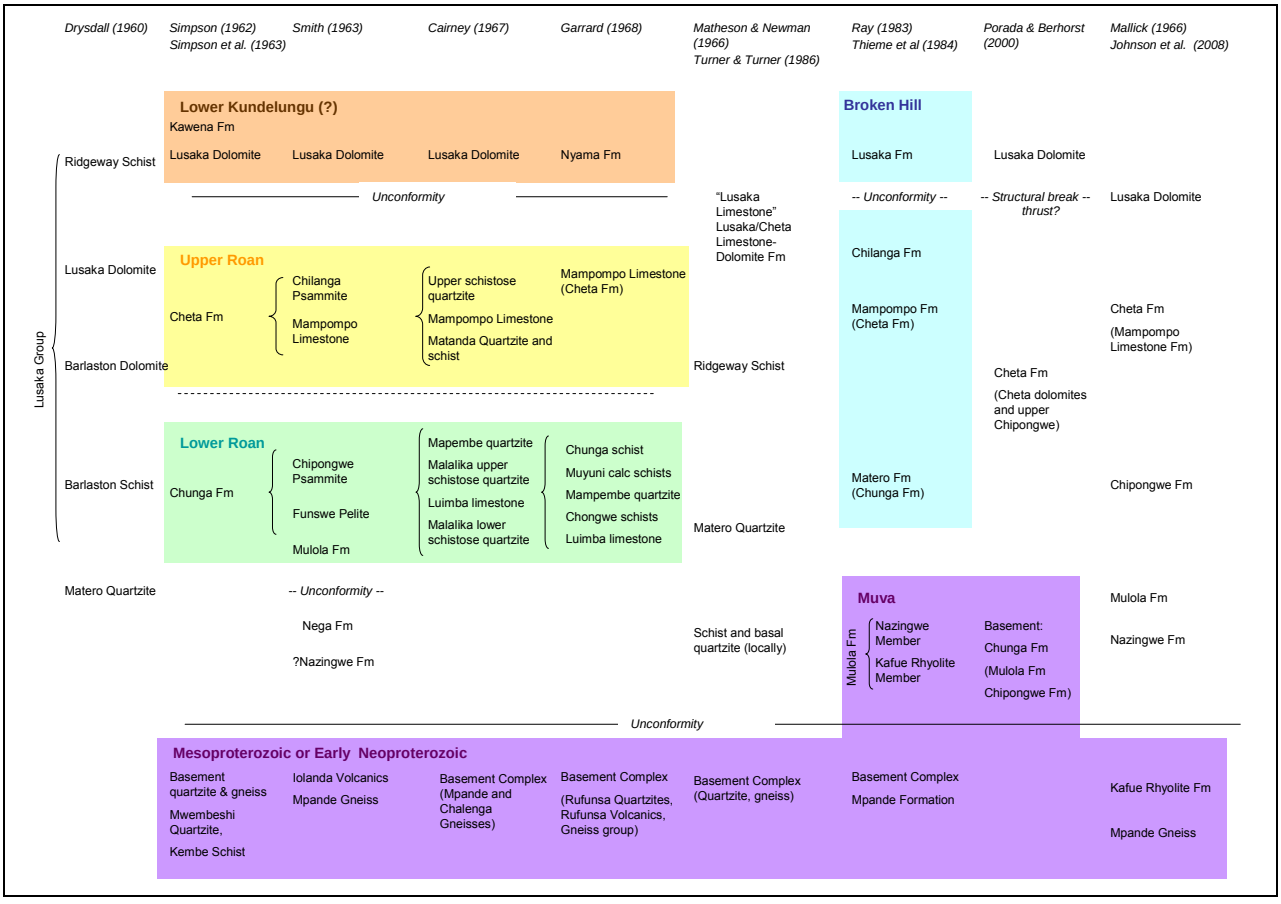

Figure 13: Stratigraphical classification of the rocks of the Zambezi supracrustal sequence and underlying basement rocks according to various authors (Bäumle & Kang’omba, 2009).

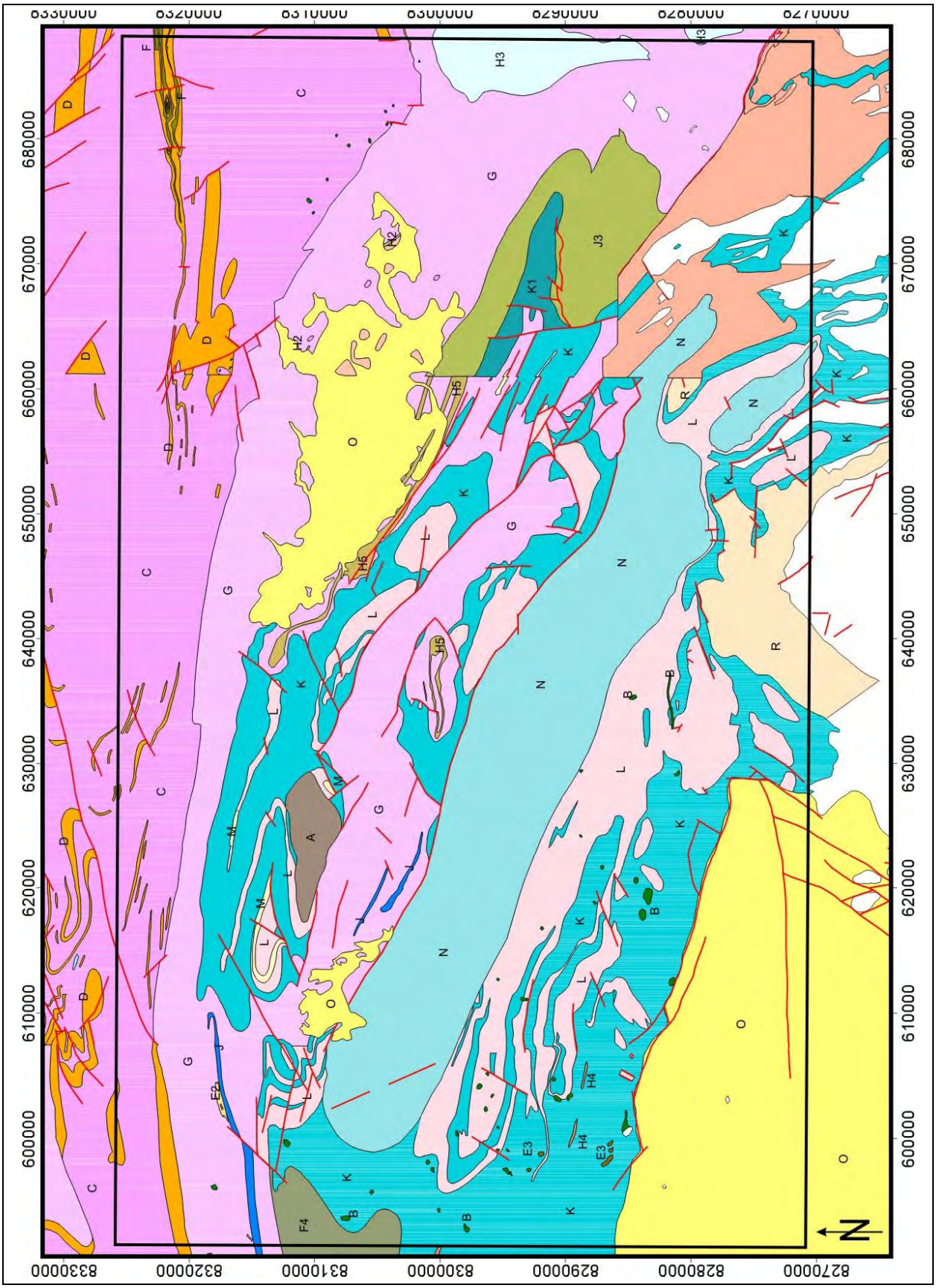

Figure 14: Adjusted and slightly simplified geological maps after Simpson et al. (1962, 1963) and Garrard (1968). The map sheet borders still show an insufficient fit due to different interpretations / terminologies for geological units.

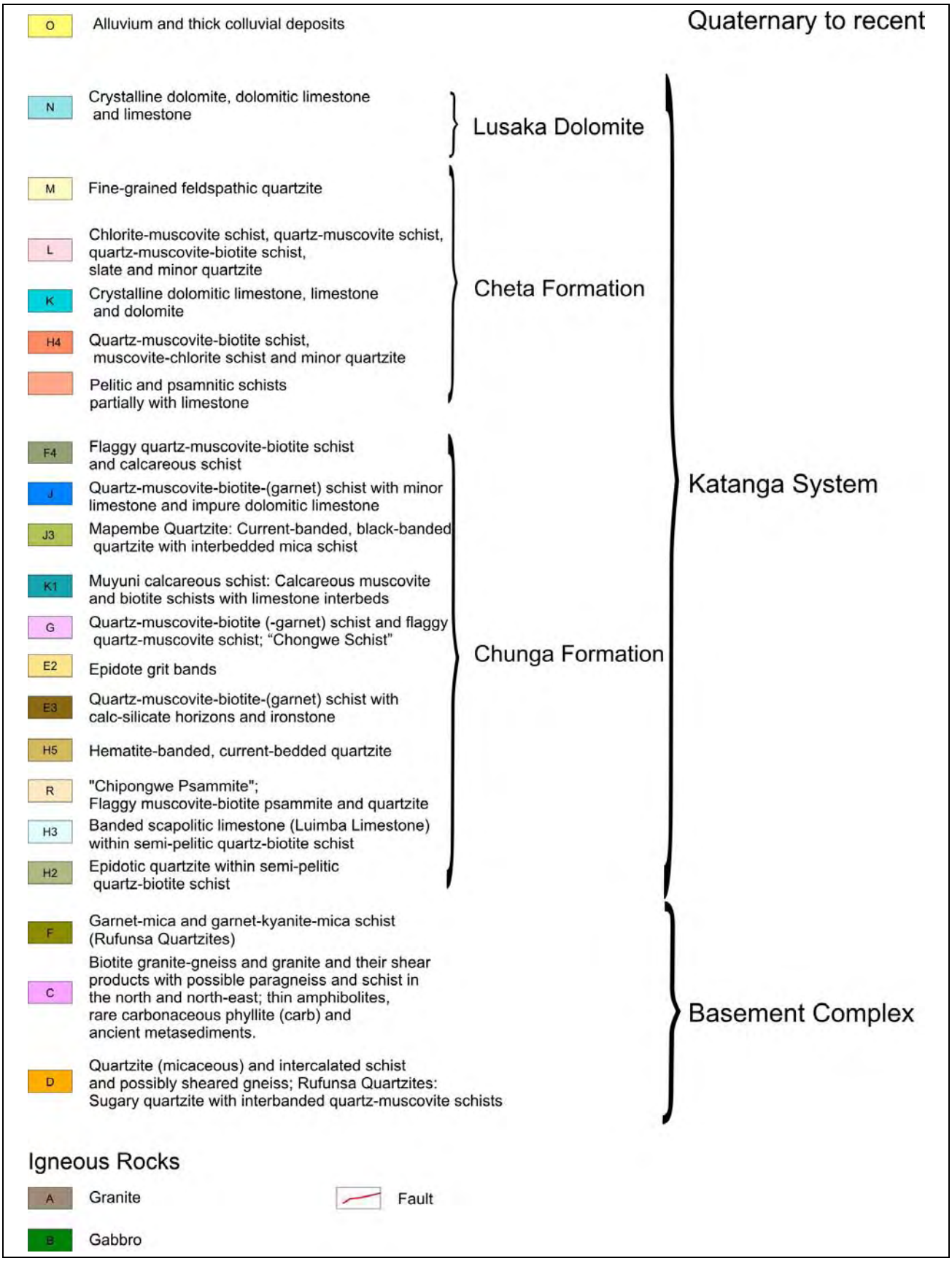

Figure 15: Legend for adjusted and slightly simplified geological maps after Simpson et al. (1962, 1963) and Garrard (1968).

5.1 Chunga Formation

Simpson et al. (1963) describe the Chunga Formation as a sequence of schists, psammites, quartzites and to a minor extent calcareous horizons, which unconformable overlies the basement. The most common lithology is a quartz-muscovite-biotite schist.

In the western part of the working area along the banks of Chunga River (WP 027) as well as in the eastern part along the banks of Kapwelyonga River (WP 132) a meta-basalt-like rock type occurs. It is a dark grey, dense and heavy material, with a homogenous look. At Chunga River this rock type shows a strong chloritisation, which is common for hydrothermally altered basic rocks (figure 16).

In the field, the schists and quartzites typically form prominent ridges. Quartz-muscovite-biotite schist often reveals a fine lamination (figure 17).

Calcareous horizons within Chunga quartzite have the same shape as most calcareous units in the Cheta Formation (figure 18).

Figure 16 left: Meta-basalt-like rock type of Chunga Formation at Kapwelyonga River (WP 132). Right: the same rock type at Chunga River shows a strong chloritisation (visible by green colour of new formed chlorite), which is typically for hydrothermally altered mafic rocks (WP 027).

Figure 17: Typical quartz-muscovite-biotite schist of Chunga Formation. Inset shows a fine lamination (WP 123).

Figure 18: Calcareous horizon within Chunga quartzite. Inset shows a coarse grained crystalline limestone (WP 121).

5.2 Cheta Formation

According to Simpson et al. (1963) the Cheta Formation consists of two calcareous- and two schist members. It is however unknown if this is a true stratigraphical sequence or a repetition due to early recumbent folding. Limestones of the calcareous horizons range from pure dolomite to pure limestone (Simpson et al. 1963).

In the working area their colours range from white to grey and grain sizes from fine (< 1 mm) to very coarse (5 mm to 10 mm, figure 19). Coarse grains seem to occur, where stronger deformation and/or vicinity to the granite body may have initiated recrystallisation and grain growth. Within the calcareous horizons, layers of more siliceous content occur. They are grey and white laminated and contain muscovite (figure 20).

Figure 19:
Karstified limestones of the Cheta Formation. Insets show coarse grain sizes with crystals up to 10 mm (WP 104 above and WP 078 below).

Figure 20: Hard siliceous horizon within limestone unit of Cheta Formation with no visible karstification. Inset shows altered muscovite in brownish colour (WP 098).

The schists typically form prominent ridges. They include rock types like quartzites, quartz-muscovite-chlorite schists and quartz-muscovite schists. The quartz-muscovite schists found in the working area were fine grained with muscovite accumulated on cleavage planes (figures 5 and 21, WP 066 and WP 069) and with primary sedimentary structures like channel deposits (figure 21, WP 075). The colours range from white and pink to grey, at some locations with iron-oxide-spots. The schists are similar to those of the underlying Chunga Formation.

At some locations, the laminated schists are directly underlain by horizons of pure milky opal (figure 22).

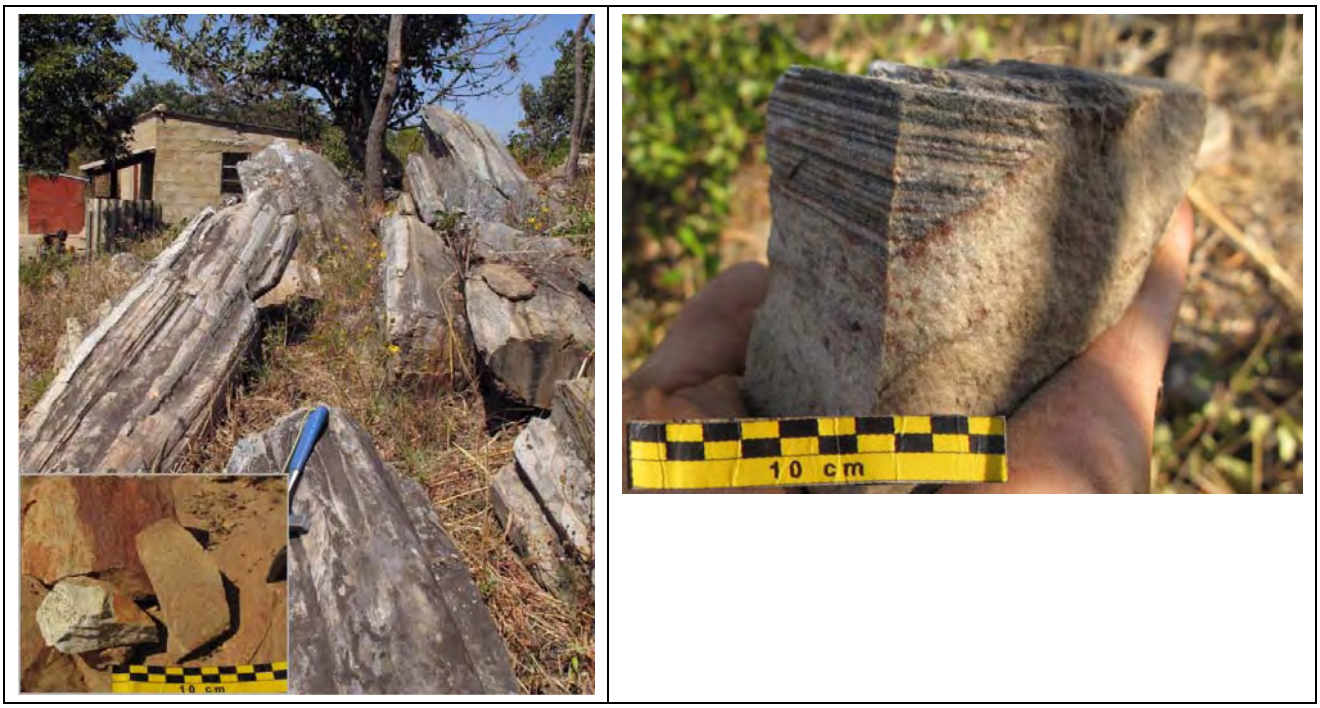

Figure 21: Left: schists of the Cheta Formation. Inset shows white fine grained quartz-muscovite schist with muscovite accumulated on cleavage planes. (WP 066 and inset WP 069). Right: fine laminated channel deposit with spots of iron-oxide (WP 075).

Figure 22: At some locations pure milky opal forms thick horizons which underlie the schists (WP 081).

5.3 Lusaka Dolomite Formation

Simpson et al. (1963) postulate that the younger Lusaka Dolomite Formation unconformably overlies the older Cheta- and Chunga Formations or was overthrusted over them at low angles as a nappe. The Lusaka Dolomite Formation exhibits layer thickening and partially underlies older schists which can also be attributed to recumbent folding (Nkhuwa, 1996).

In the working area, the colours change from pure white to light grey. Also a banding of white and grey- as well as white and pink layers is typical. The banding can often be attributed to primary layering. Besides a change in colour a change in composition towards more siliceous material can be observed (figures 23, 24, 25, 26). Grain sizes – in contrast to Chunga- and Cheta Formations – are predominantly fine.

Figure 23: Fine grained pink and white Lusaka Dolomite (WP 001).

Figure 24: Grey and white laminated Lusaka Dolomite with internal folds (WP 022).

Figure 25: Grey and white laminated Lusaka Dolomite with internal folds consisting of siliceous material (WP 063).

Figure 26: Steep dipping grey and white laminated Lusaka Dolomite with lenticular remains of siliceous material (WP 032).

5.4 Cenozoic

Colluvial deposits overlie the area around the prominent quarry of lake Ngwenya south of the city centre.

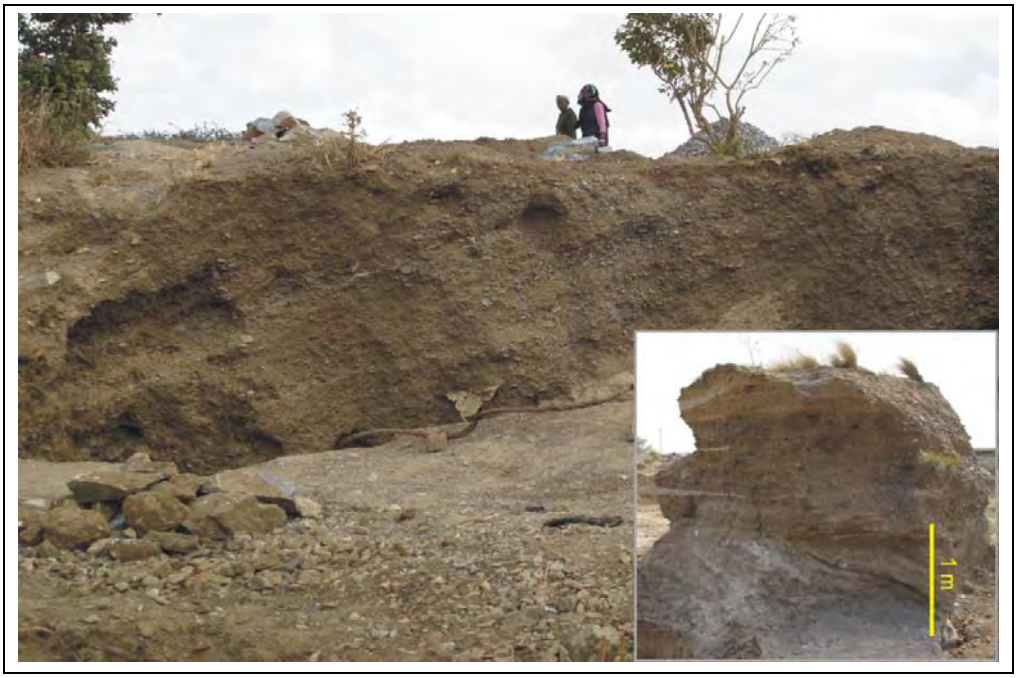

Figure 27: Inclined and horizontal breccia-like colluvial deposits at Lake Ngwenya (WP 012).

They are consisting of unsorted but layered breccia, presumably deposited by sheet floods into a local depression of a huge sinkhole (figure 27). This kind of deposition is common on gently inclined plains within the tropic zone of alternating rainfalls.

5.5 Soil

A variable thickness from a few decimetres up to ± three metres of pisolititic plinthosol, which developed on the Lusaka Dolomite Formation and calcareous horizons of the Cheta Formation, can be observed (figures 28 and 29). The soil colour ranges from red to brown and mainly depends on the content of iron oxides.

In some places a considerable amount of dispersed magnetite is also present in the plinthosol (figure 30).

A second soil type, which developed on calcareous units, is so called “black soil” (figure 31). It contains more clay and humus and is used as a fertile substratum for gardens. In the southern part of the Lusaka Plateau black soil is underlain by

1. fine grained, light grey/greenish “building sand”, which contains clay minerals (figure 32) and
2. coarse grained “river sand”. Both types are used for construction purposes.

Sandy soils, which developed on schists and on Lusaka Granite NW of Lusaka, are used for constructions as well (figure 33). All terms in quotation marks are local expressions.

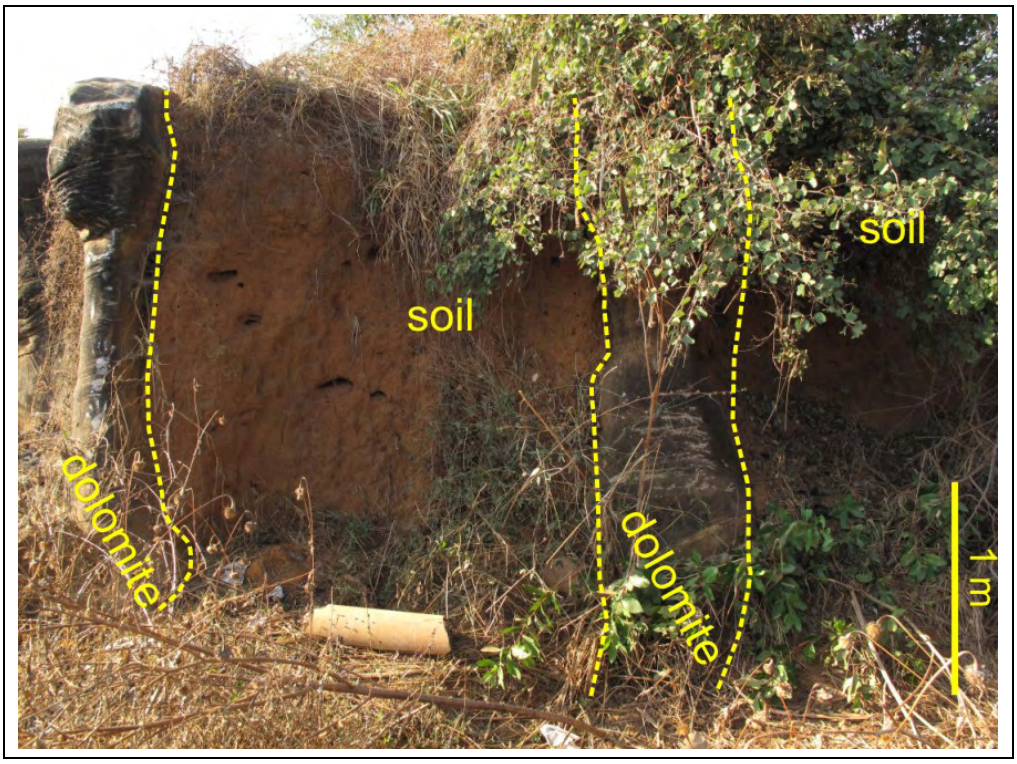

Figure 28: Plinthic soil between solution pillars of Lusaka Dolomite (WP 063).

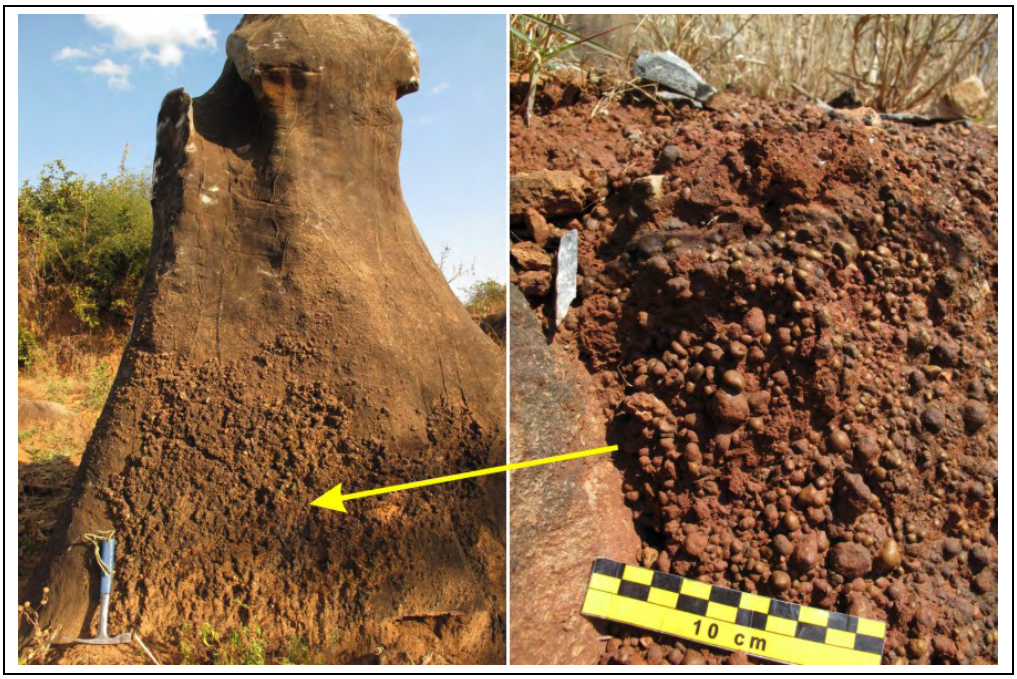

Figure 29: Left: Solution pillar of Lusaka Dolomite with remains of pisolitic plinthosol (WP 063). Right: close up of similar pisolitic plinthosol from location of WP 031.

Figure 30: Dispersed magnetite in plinthic soil sticking to a magnet (WP 034).

Figure 31: “Black soil” used as a fertile substratum for gardens on a transporter at southern Lusaka Plateau (WP 033).

Figure 32: In foreground “building sand” near a borehole at southern Lusaka Plateau (WP 035).

Figure 33: One of several sand quarries in soil of Lusaka Granite NW of Lusaka. View from WP 083, 500 metres towards 100°.

6 Karstification

Karstification is a common feature of all calcareous units of the working area. Karst holes are usually filled with soil. At populated places, the soil cover often is removed to get either soil or limestone for building purposes. Places of such small unofficial quarries are easily detectable in high resolution satellite imagery as all medium-sized karst structures are enhanced (figure 34).

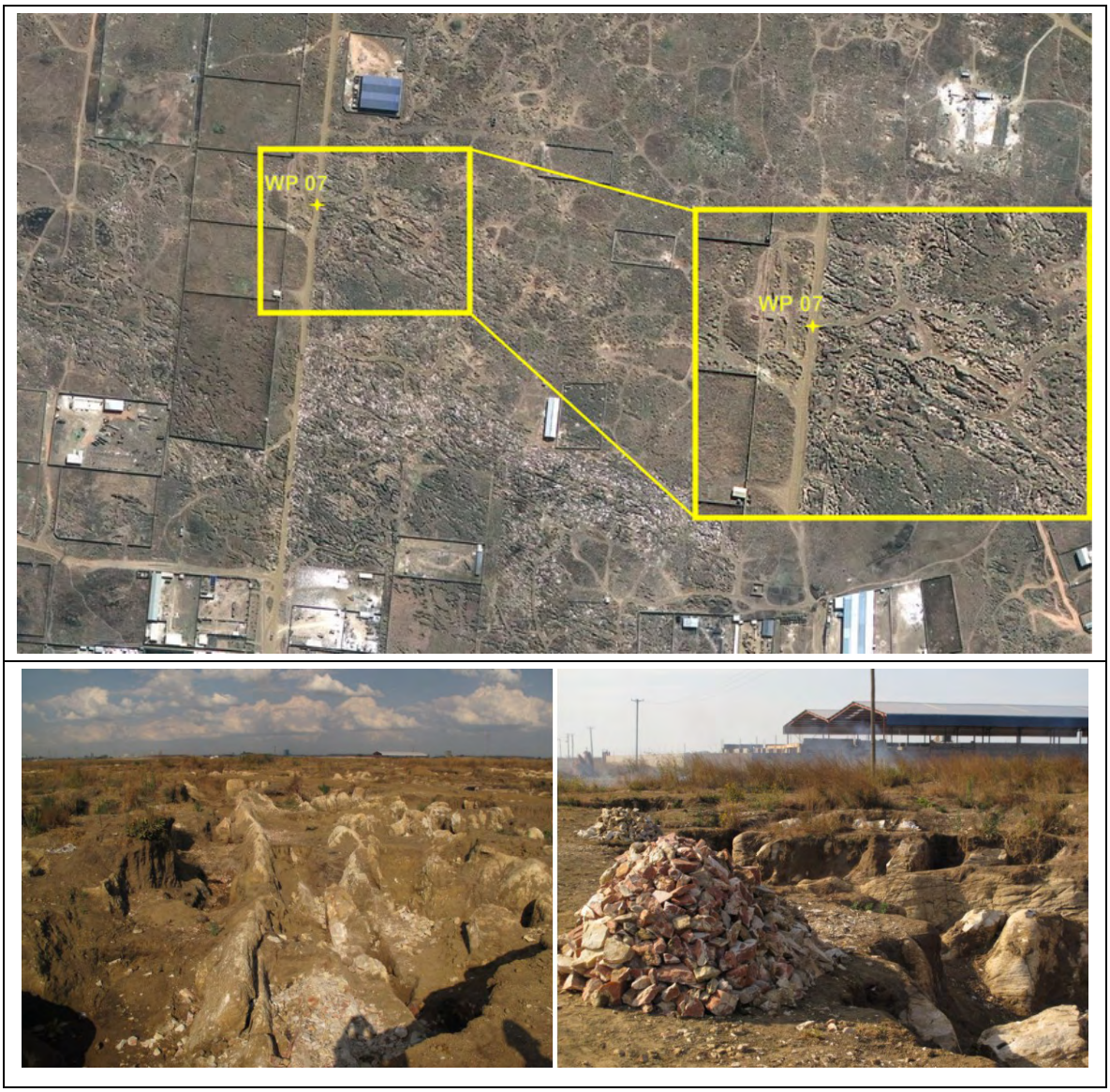

Figure 34: Above: removed soil from Lusaka Dolomite enhances the karst structures of that formation. Inset shows a close up of the area of ground check at WP 007 west of the city. High resolution Quickbird Image from “Google Earth”, acquisition date: July/12/2009. Below: Field photos of that area show karst features. Left: view to SE along structural trend. Right: small unofficial limestone quarry to fetch material for construction purposes.

There are different dimensions of karstification ranging from micro karst of calcareous surfaces to karst holes of several metres in width (besides “mega” karst features like sinkholes, which are not described in this report). As most karst features have been formed along strike of geological structures, the lengths of holes usually are taller than widths but can not be followed in most

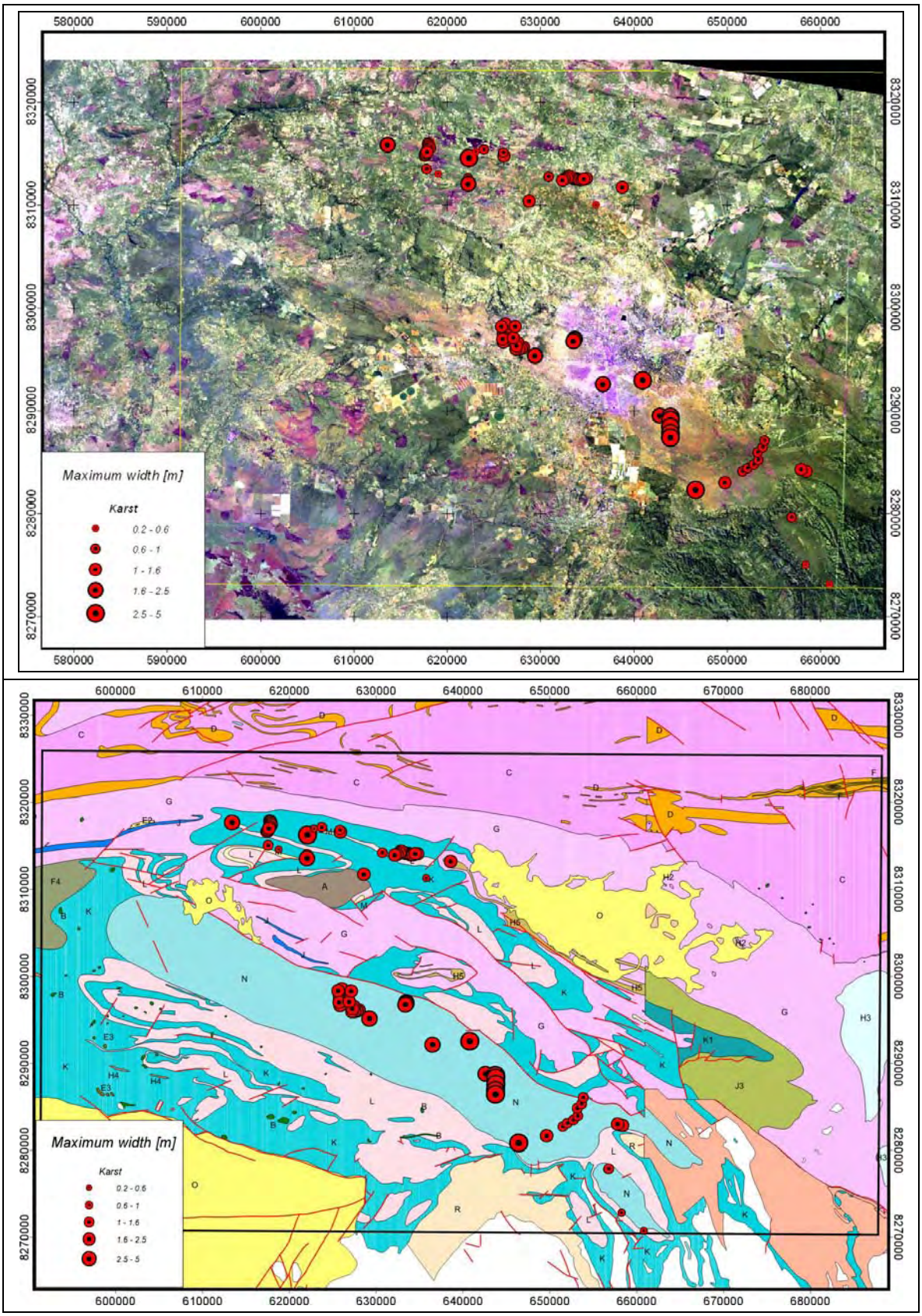

Figure 35: Maximum widths of karst features in the working area. Above: Allocation of checked karst features projected into Landsat ETM image bands 7,4,2 (RGB). Below: Allocation of checked karst features projected into adjusted and slightly simplified geological maps after Simpson et al. (1962, 1963) and Garrard (1968) for legend see figure 15.

locations due to thick soil and vegetation cover. For that reason figure 35 concentrates on the description of maximum widths, ignoring (larger) lengths.

The next figures show examples of the karst dimensions at the checked outcrops. The working area was thus subdivided in three areas A, B and C (figure 36). Each of them is then shown in a closer view with locations of the following field photos (figures 37 to 61).

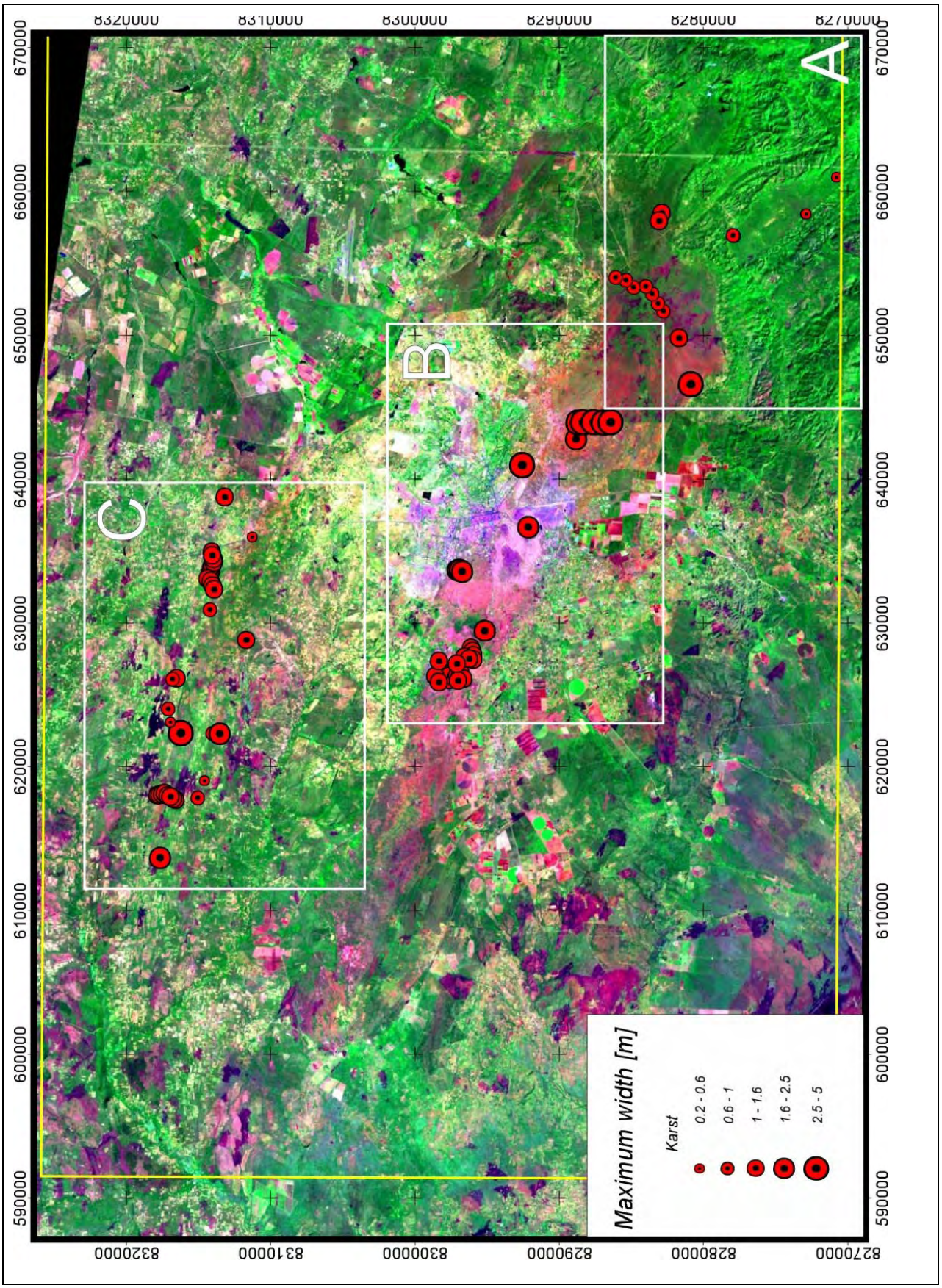

Figure 36: Overview of karst dimensions and locations of subdivided karst areas A, B and C.

6.1 Karstification area A

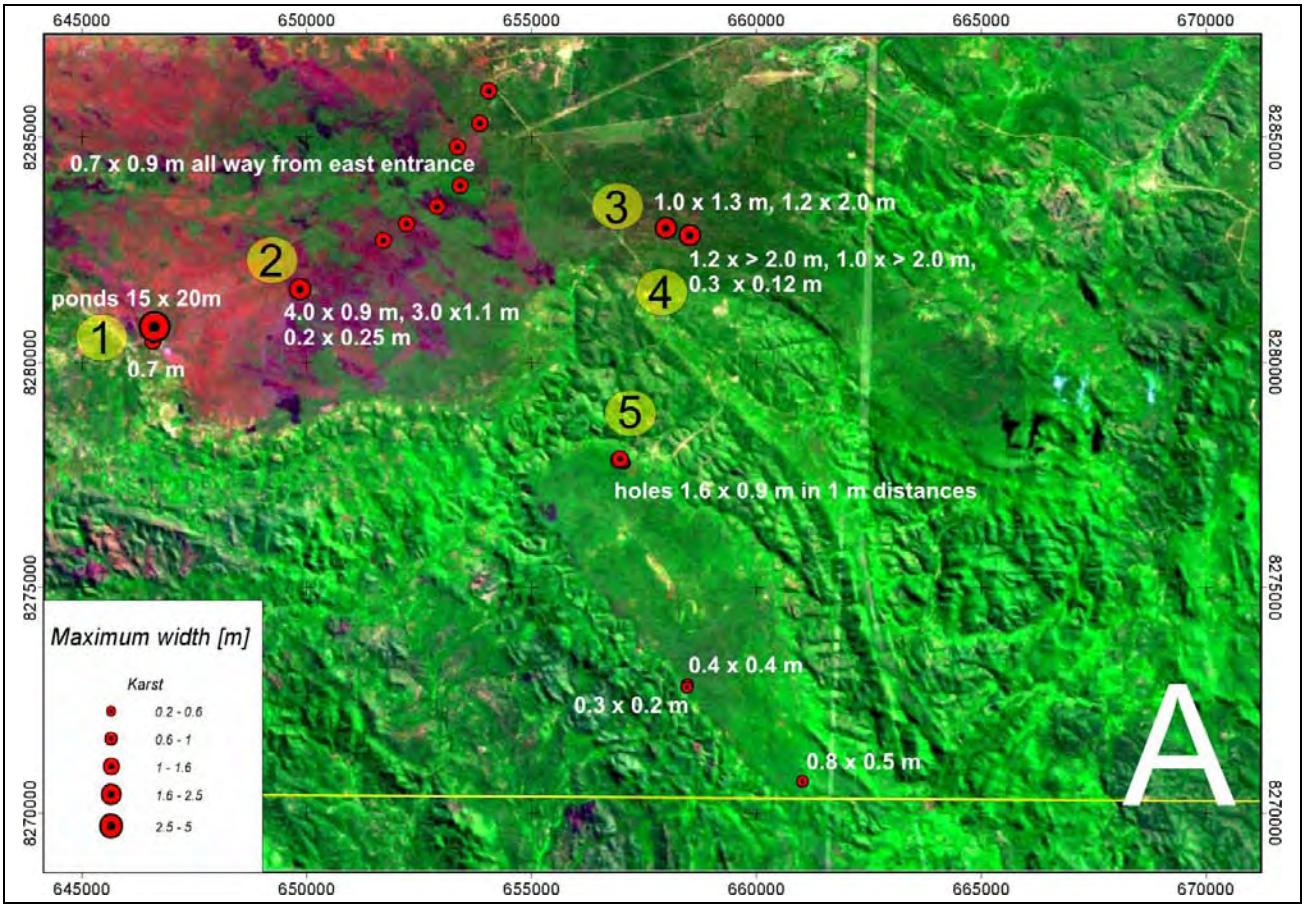

Figure 37: Overview of karst area A. Yellow numbers mark locations of field photos.

Figure 38: Solution pillars with micro karst on surfaces confining small ground water-filled ponds where soil was removed (WP 062).

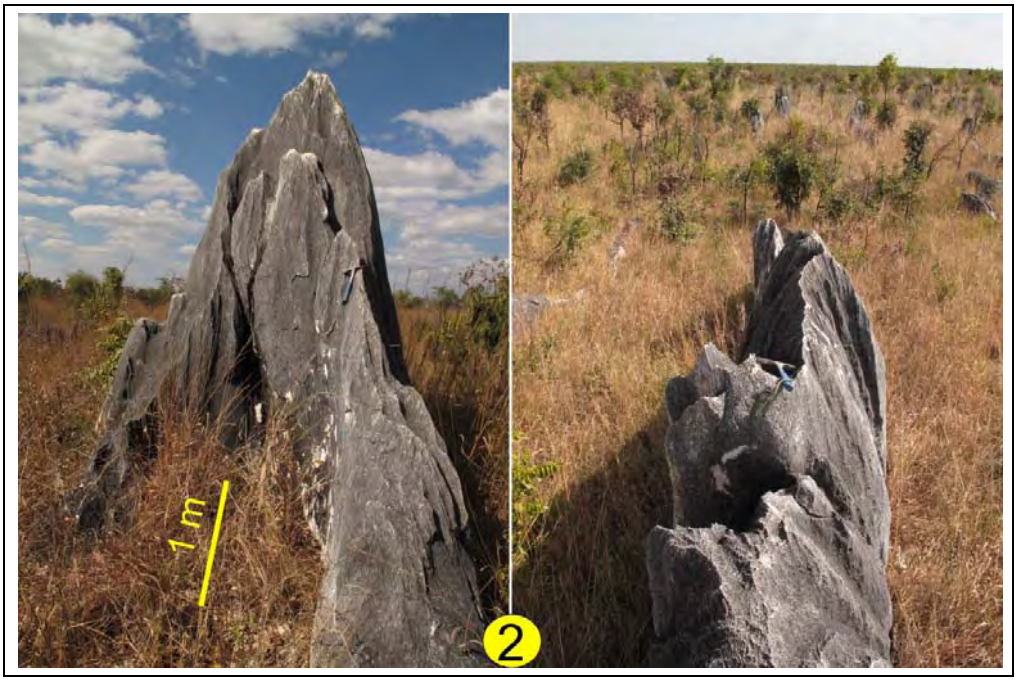

Figure 39: Pinnacle karst up to 5 metres high in the area of Lusaka South Local Forest (WP 060).

Figure 40: Panoramic view over pinnacle karst and scrubland (WP 060 from 130°-260°).

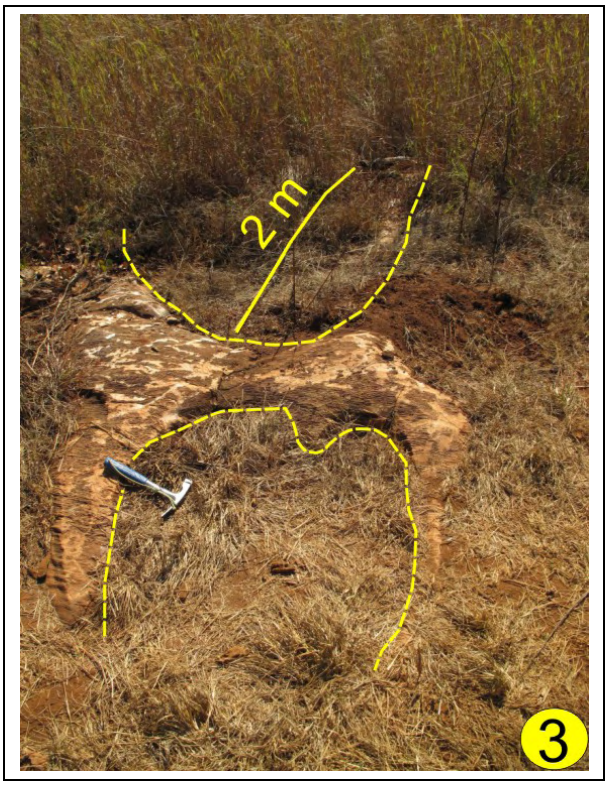

Figure 41: Soil-filled karst holes (WP 054).

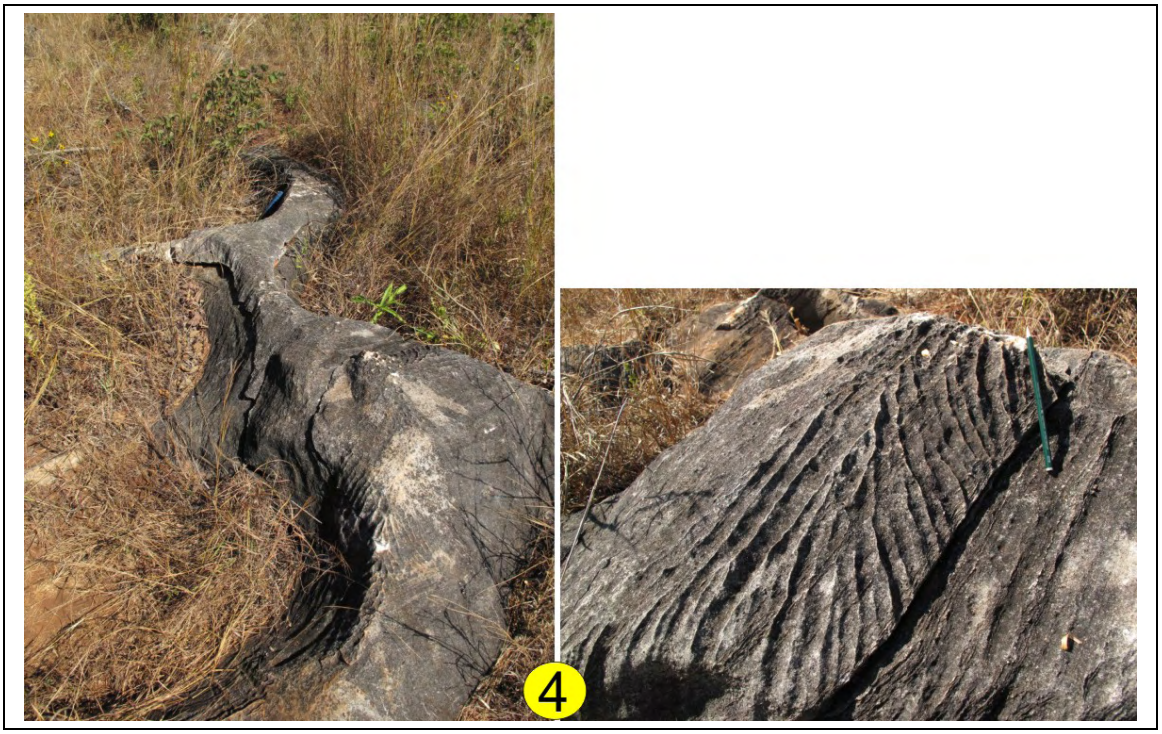

Figure 42: Soil-filled karst holes and micro karst on surface of Lusaka Dolomite (WP 053).

Figure 43: Soil-filled karst holes (WP 043).

Figure 44: Steep layers of Lusaka Dolomite with micro karst along layering (WP 042).

6.2 Karstification area B

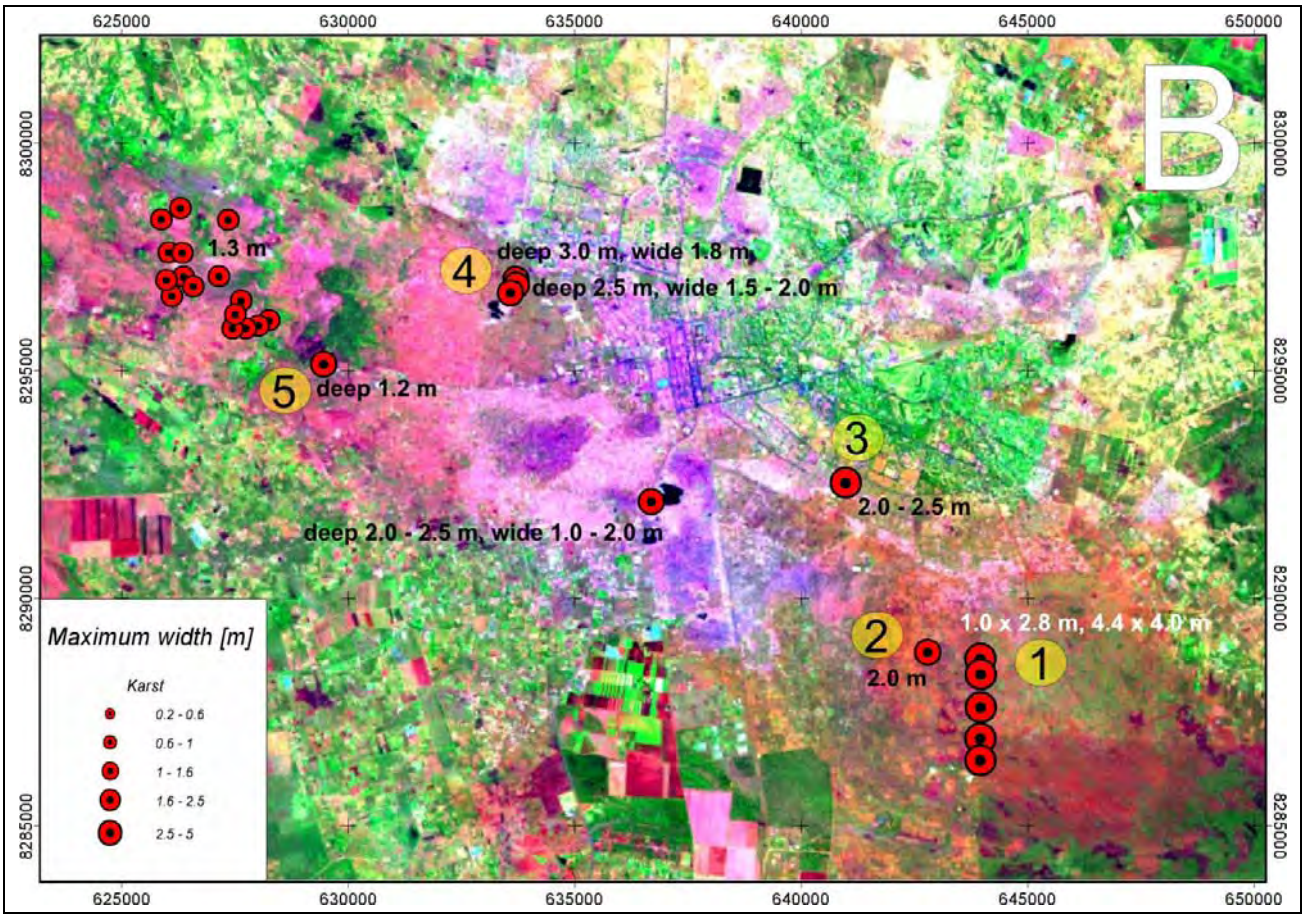

Figure 45: Overview of karst area B with Lusaka in the centre. Yellow numbers mark locations of field photos.

Figure 46: Large soil-filled karst holes in development area. View to 170° (WP 111).

Figure 47: Small karst holes and micro karst in Lusaka Dolomite. Pinnacle karst with heights from 0.3-2.5 metres (WP 029).

Figure 48: Solution pillars in Lusaka Dolomite. Plinthic soil was removed (WP 063).

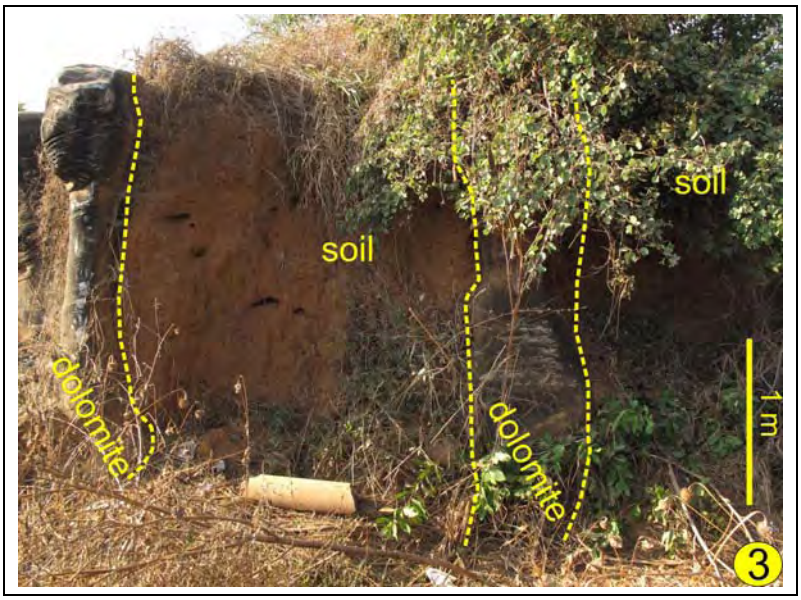

Figure 49: Solution pillars in Lusaka Dolomite with plinthic soil (WP 063).

Figure 50: Water-filled karst hole; 2.5 metres deep (WP 006).

Figure 51: Soil-filled karst holes between steep layers of Lusaka Dolomite in development area (WP 008).

6.3 Karstification area C

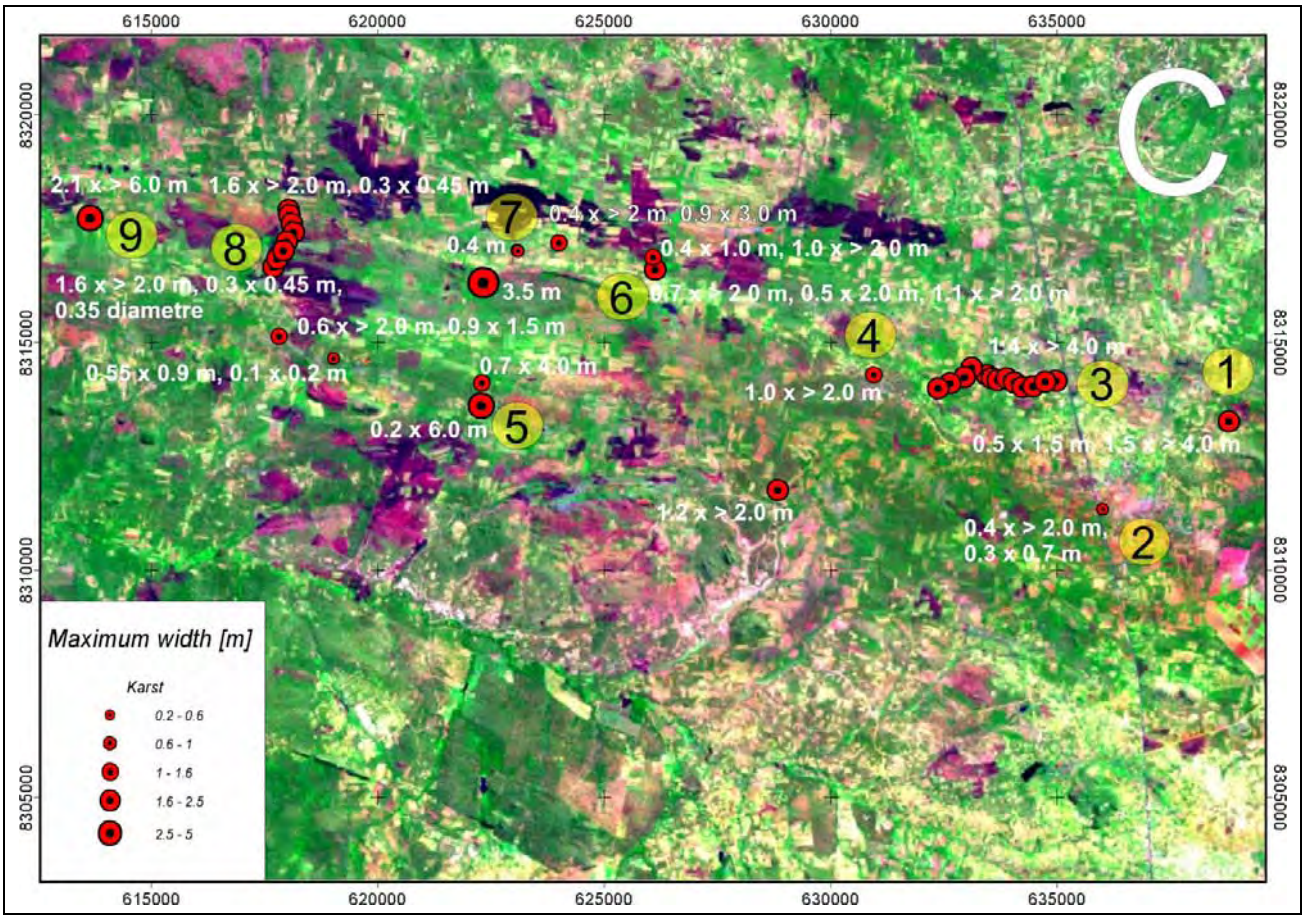

Figure 52: Overview of karst area C. Yellow numbers mark locations of field photos.

Figure 53: Soil-filled karst holes in calcareous horizon of Chunga Formation (WP 121).

Figure 54: Soil-filled karst hole of Cheta Formation at drilling site no. 28 (WP 065).

Figure 55: Soil-filled karst hole of Cheta Formation (WP 128).

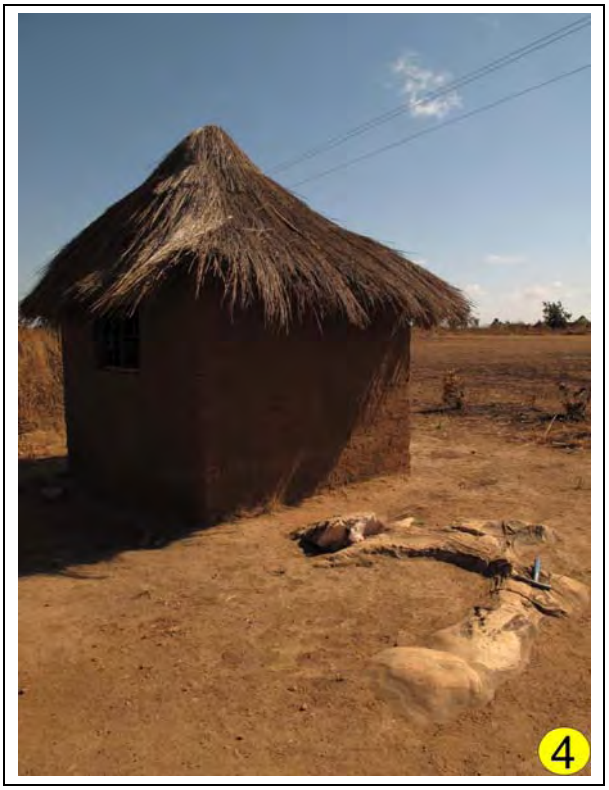

Figure 56: Soil-filled karst hole of Cheta Formation (WP 088).

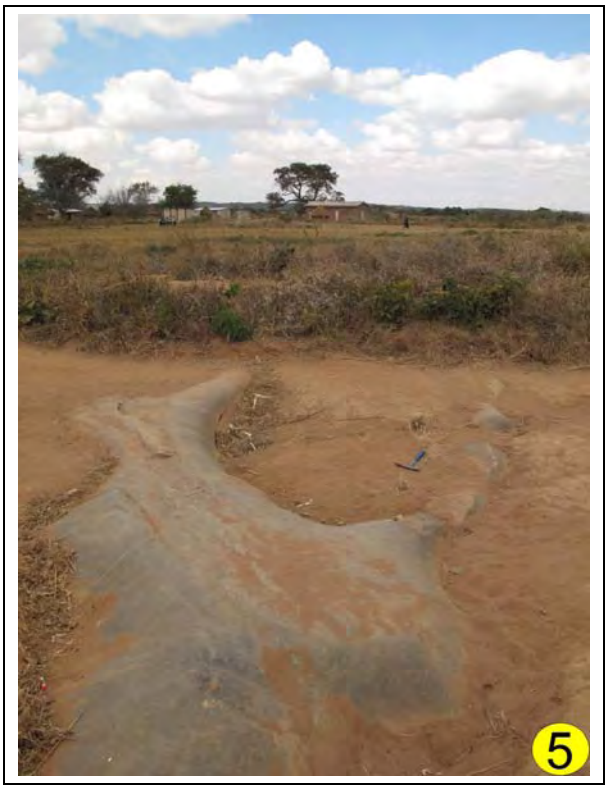

Figure 57: Soil-filled karst hole of Cheta Formation (WP 095).

Figure 58: Soil-filled karst hole of Cheta Formation (WP 078).

Figure 59: Horizontal karst channels of Cheta Formation; above: WP 091, below: WP 090.

Figure 60: Soil-filled karst hole of Cheta Formation (WP 104).

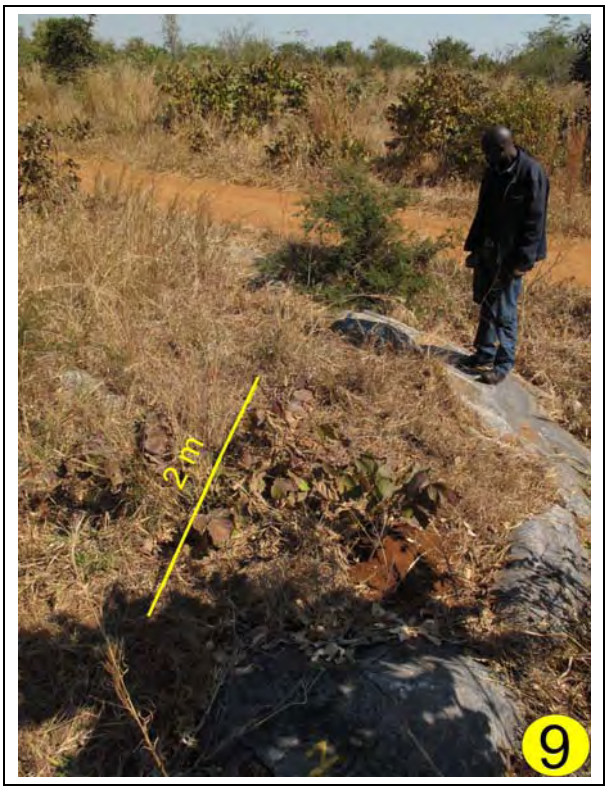

Figure 61: Soil-filled karst hole of Cheta Formation (WP 113).

6.4 Possible water contamination

Karst aquifers are exceptionally vulnerable to pollution. Large cavities cause a fast ground water flow which anticipates filter effects.

In the working area there are plenty sources for possible contamination. Besides the “usual” problems of a big and densly populated city such as traffic and seepages from gas stations, there are local sources like

- Unofficial dumping and
- Pit latrines,

which can cause direct problems for the very neighbourhood.

Figure 62: Local water supply of a compound may be affected by ground water contamination from dumping and pit latrines nearby (WP 013).

Figure 63: Pit latrines discharging directly into karst holes (WP 016).

Figure 64: Dumping in karst area of Lusaka Dolomite can cause ground water contamination. Left: WP 016, right: WP 009.

7 Land use

An automated supervised classification was carried out with the method “maximum likelihood” of 80 %. As a data base for that purpose, a Landsat ETM scene with acquisition date May, 13, 2002 was chosen.

The following seven classes were defined (figure 65):

- Water,
- Settlement,
- Bare soil plinthic,
- Bare soil plinthic 1,
- Bare soil,
- Agriculture and
- Forest.

For reasons of topicality, the classes

- Water, settlement, agriculture and forest

were then manually adjusted in a GIS on basis of four SPOT scenes with acquisition dates July, 11, 2008 (western part), August, 13, 2007 (north east), July, 14, 2007 (south east).

Some classes could not be created accurately with available data, using an automated classification. This is because of

1. limited spectral information,
2. overlapping features e.g. vegetation of small scale agriculture and garden plots with scrubland, or
3. ambiguous spectral features from the same class e.g. fallow- and cultivated small scale agriculture,
4. fallow small scale agriculture interferes with the classes of different kinds of bare soil.

For these reasons, three additional classes

- small scale agriculture
- settlement with garden plot and
- scrubland

were defined and displayed as raster data with accordant legends (figure 66, 67).

The classes “Bare soil plinthic” and “Bare soil plinthic 1”, could have been combined in one class. As they are spectrally well discriminable (most likely due to different contents of iron and organic matter), it was preferred to display these areas as separate classes.

From 2002 to recent the most striking change is a loss of forest and scrubland in favour of commercial- small scale agriculture, as well as for the production of charcoal (figures 68-78). Also development areas are growing rapidly, especially in the south of Lusaka.

Due to limited schedule, only a minor number of agricultural areas could be checked in the field. At those locations, the main cultivated crops were:

Commercial agriculture (figures 71, 72) :

- maize
- wheat
- pepper and to a minor extent
- banana

Small scale agriculture (figures 68-70):

- maize in combination with pumpkin
- okra
- cabbage
- sweet potatoes and
- cotton

7.1 Creation of the Generalized Landuse Map

Using the seven classes generated by the automated supervised classification from the Landsat ETM scene acquired in May, 2002, a generalized land use map at scale 1:200,000 was created. The classes generated are namely (see Chapter 7 above):

- Water,
- Settlement,
- Agriculture,
- Forest
- Bare soil

- Bare soil plinthic
- Bare soil plinthic1

The landuse map is supposed to give an impression of the spatial variability of major different land use types in the project area at the desired scale. Therefore the originally generated classes had to be generalized.

The generalization of the land use pattern in the study area included the following steps:

- Deleting features of very small areas: a minimum threshold in area had to be fixed in order to clean out the map. A general threshold of two hectares was fixed for the forest, scrubland and bare soil patches.
- Combining the two different plinthic soil types (‘baresoil plinthic’ and ‘baresoil plinthic1’) into one class (‘baresoil plinthic’).
- Prioritizing in case one land use feature partially overlapped another. In such cases the class types were prioritized as follows: water – settlement – agriculture – forest – bare soil classes, in this order. (e.g. agriculture could not be underlain by say bare soil, and overlapping areas would be deleted accordingly.)
- Defining and digitizing three additional classes features with mixed land use, namely ‘scrubland’, ‘settlement with garden plots’ and ‘small scale agriculture’. The digitizing was done to best possible accuracy but arbitrarily based on the processed Landsat ETM scene.

Throughout this whole exercise, the most recent Google earth images of the project area acquired on 26th May, 2010 was overlain. This was also in order to assist in verifying the land use types.

All of these nine classes were then merged in GIS into one layer hence making up the land use map included in the Appendix.

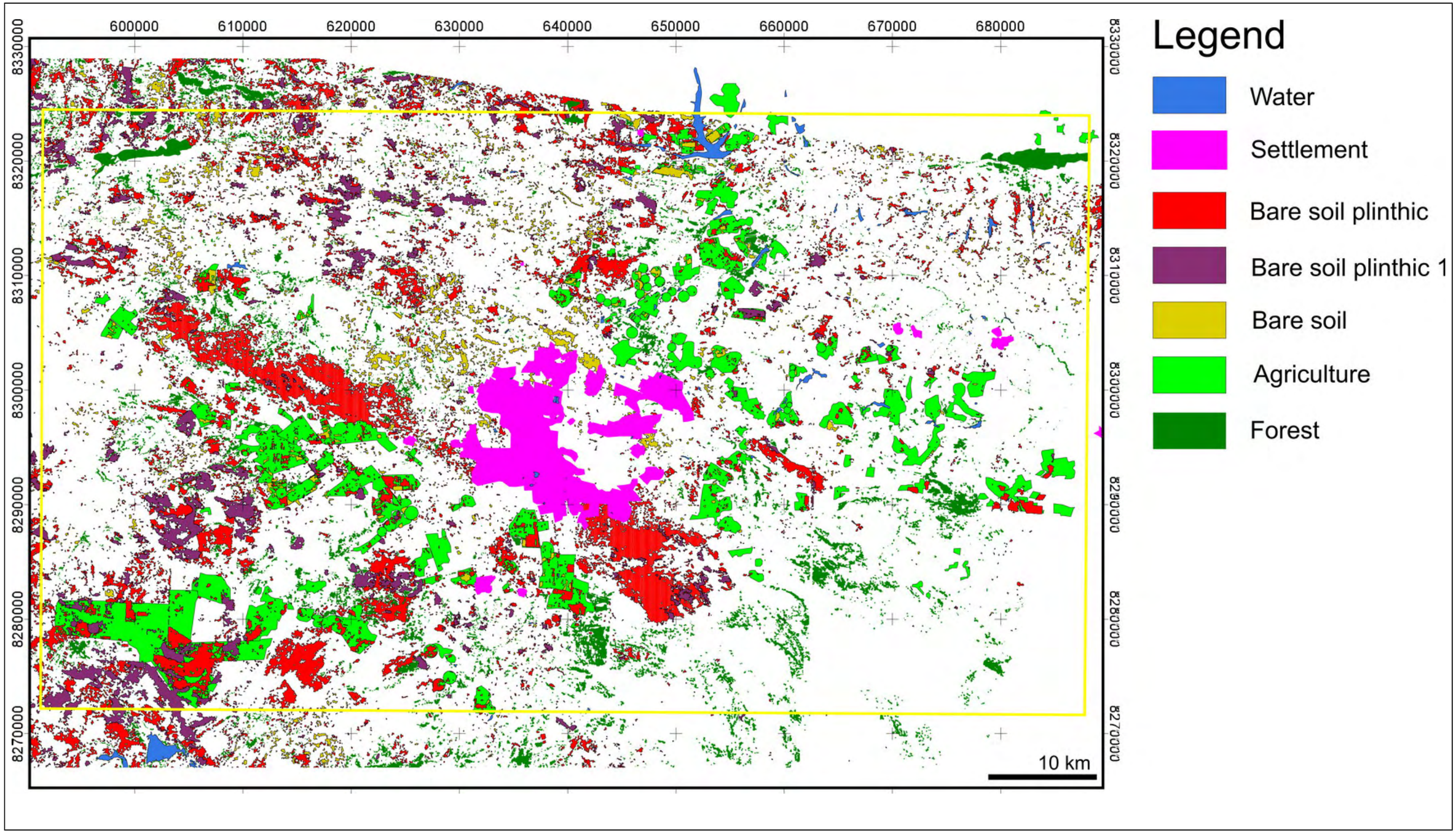

Figure 65: Classification result on basis of 2002 Landsat ETM scene manually adjusted in recent (2007 and 2008) SPOT scenes.

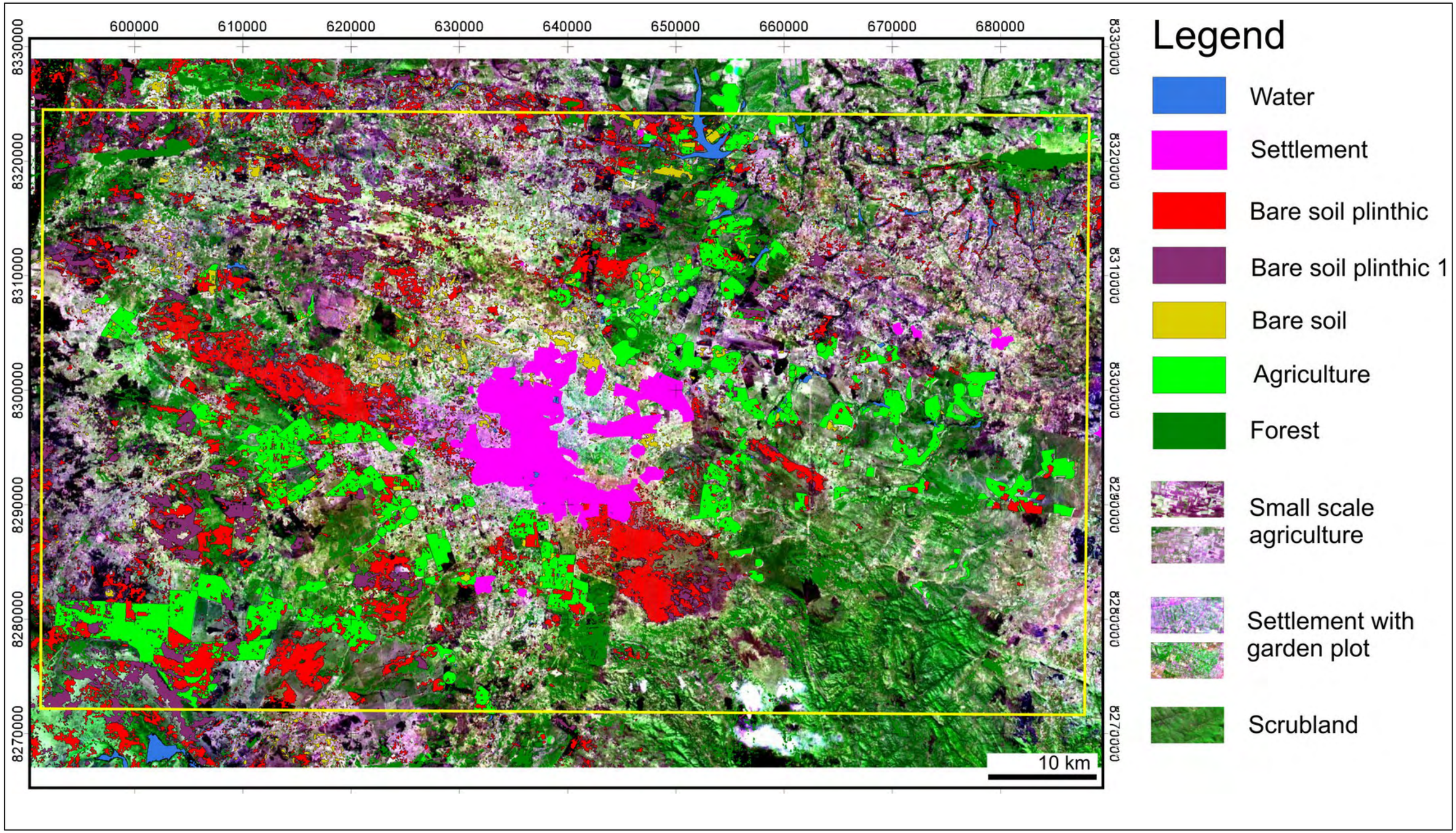

Figure 66: Classification result on basis of 2002 Landsat ETM scene manually adjusted in recent (2007 and 2008) SPOT scenes projected into SPOT. Additional classes of “small scale agriculture”, “settlement with garden plot” and “scrubland” can be pointed out using the raster image legend.

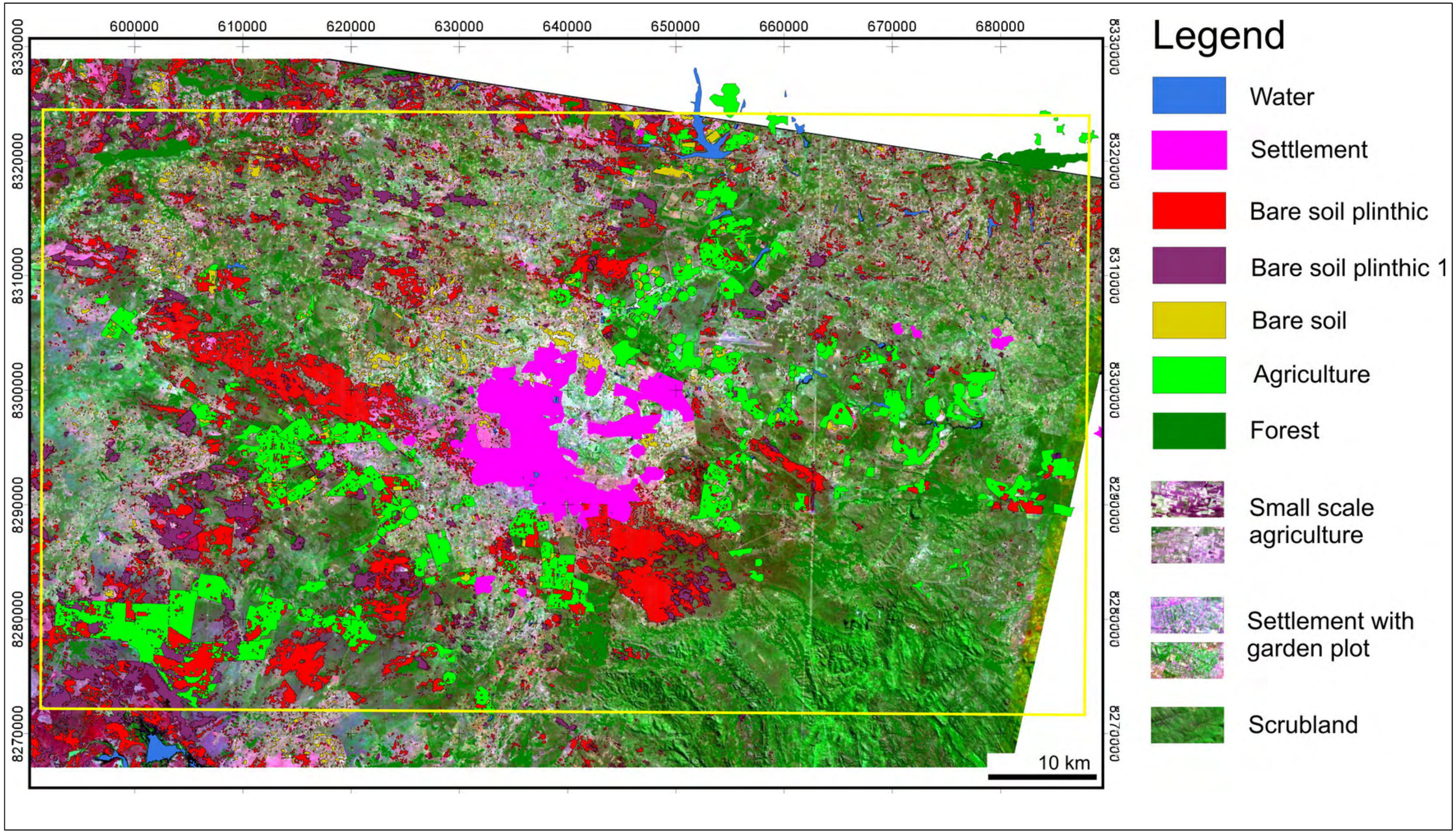

Figure 67: Classification result on basis of 2002 Landsat ETM scene manually adjusted in recent (2007 and 2008) SPOT scenes projected into Landsat ETM. Additional classes of “small scale agriculture”, “settlement with garden plot” and “scrubland” can be pointed out using the raster image legend.

Figure 68: Small scale agriculture. Left: traditional village with maize field (east of WP 081). Right: Field with maize and pumpkin (WP 046).

Figure 69: Small scale agriculture with cabbage field south of Lusaka (WP 022).

Figure 70: Small scale agriculture. Above: Field with sweet potatoes close to WP 043. Below: cotton field NW of Lusaka.

Figure 71: Commercial agriculture. Above: harvested maize field. Below: wheat field (WP 055).

Figure 72: Commercial agriculture. Pepper field at Chongwe River bridge.

Figure 73: Scrubland less affected by human activity. Above: view to S of Lusaka Plateau from WP 047. Below: View to SE from WP 077.

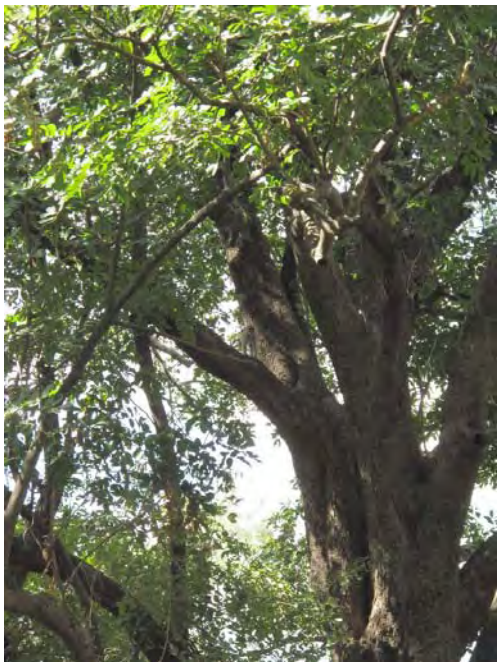

Figure 74: Small area (ca. 70 m x 70 m) of primary forest used as a cemetery within scrubland (WP 100).

Figure 75: Fire clearance for land reclamation. Above: Area NW of Lusaka view from WP 128 to SW. Below: Southern shore of Kafue reservoir. View from WP 135 to NW.

Figure 76: Charcoal production. Above: Bush cutting near WP 083. Below: Base of former charcoal kiln (burning site for charcoal production) close to WP 081.

Figure 77: Charcoal at a collection site south of Kafue dam.

Figure 78: Charcoal transport. Above: close to Chunga River bridge (WP 028). Below: 600 m NE of WP 028.

8 Conclusions

8.1 Tectonics

Three main types of joints

- Steep dipping (80° - 90° towards the NW and SE) cross joints formed perpendicular to main fold axes, with strike directions between 030° to 060°.
- Longitudinal joints parallel to the fold trends (strike 110° – 140°, dip 30 – 45° towards the SW) as well as steeply (75° to 80°) towards the NE (036° to 046°, figure 5).
- Diagonal joints striking between 150° – 180° and a minor conjugate set striking between 060° and 080°, dipping 65° to 90° to the east and south.

Three main trends/types of faults:

- Strike direction NW – SE (approx. 120°), parallel to the main structural trend,
- A further NW – SE direction (140°)
- A probably conjugate NE – SW direction (035°, 045°).

To a minor extent also a NE – SW trend (080°), paralleling the “Mwembeshi shear zone (MSZ) direction” is present (figures 7 and 8).

In satellite images to the W and NW of Lusaka – by influence of the MSZ – almost any fault of all three types shows shear lenses with a fractal pattern. E.g. lenses of 17 km length to a few metres length can be observed (figure 10).

To the SE, increasing influence of the Zambezi-rift can be observed by NE-striking normal faulting and absence of shear lenses (figure 11).

Evidence of deep approx. vertical faulting can be found along a line of talc quarries and occurrence of tall calcite crystals within the Lusaka Dolomite Formation SE of the city.

8.2 Karst features

Karstification is a common feature of all calcareous units of the working area. Karst holes are usually filled with soil. At populated places, the soil cover often is removed to get either soil or limestone for building purposes.

Due to vegetation- and soil cover, relatively few locations, compared with the whole area, could be validated in the field. All of them were found to be karstified.

As most karst features have formed along strike of geological structures, the lengths of holes usually are taller than widths but can not be followed in most locations due to thick soil and vegetation cover. For that reason the description of karst dimensions concentrates on maximum widths, ignoring (larger) lengths.

The dimensions of karst holes measured in the working area range from 0.20 m to 5 metres. It appears to be most likely, that all covered calcareous units in the working area are karstified in a similar way as at the checked outcrops.

8.3 Possible water contamination

In the working area there are plenty sources for possible contamination. Besides the “normal” problems of a big and dense populated city for example traffic and seepages from gas stations, there are local sources like

- Unofficial dumping and
- Pit latrines,

which can cause direct problems for the very neighbourhood.

8.4 Land use

From 2002 to recent the most striking change is a loss of forest and scrubland in favour of commercial- and small scale agriculture, as well as for the production of charcoal for the local market (figures 68-78). Also development areas are growing rapidly, especially in the south of Lusaka.

8.5 Remote sensing

Due to coverage of soil and vegetation, many small scale karst features were only detectable by intensive field work. Despite, usage of remote sensing techniques have been essential to

- detect karst features where soil was removed and planning ground checks at those locations,
- detect and delineate faults of different order as well as fracture systems,
- recognize structural trends due to the general perspective and large ground coverage of the sensors used,
- discriminate land use categories by means of supervised classification using multispectral data.

Faults, defining shear lenses are commonly visible by a minor change in colour, unlike those faults that have a negative topographic expression and are thus enhanced by a pattern of streams and rivers.

In the first case, it is essential to work with multispectral data, as only these data are able to enhance those subtle spectral contrasts sufficiently. Usage of multispectral Landsat ETM- and SPOT data has contributed to a more detailed structural inventory of the working area.

Finally it must be stressed, that proper field work in combination with remote sensing techniques yields best results for understanding geology and tectonics with all their correlations in a defined working area.

8.6 Recommendations and open questions

Joints

Joints in calcareous formations appear to be filled with calcite in most locations and thus could be considered to be tight for ground water migration. On the other hand the calcitic fill of joints is dissolved relatively fast and acts as a nucleus for the development of karst holes.

Joints of schist formations appear to be open in most locations and thus could be considered to act as pathways for ground water migration. Both observations were not pursued systematically in the field and could be subject for further investigations.

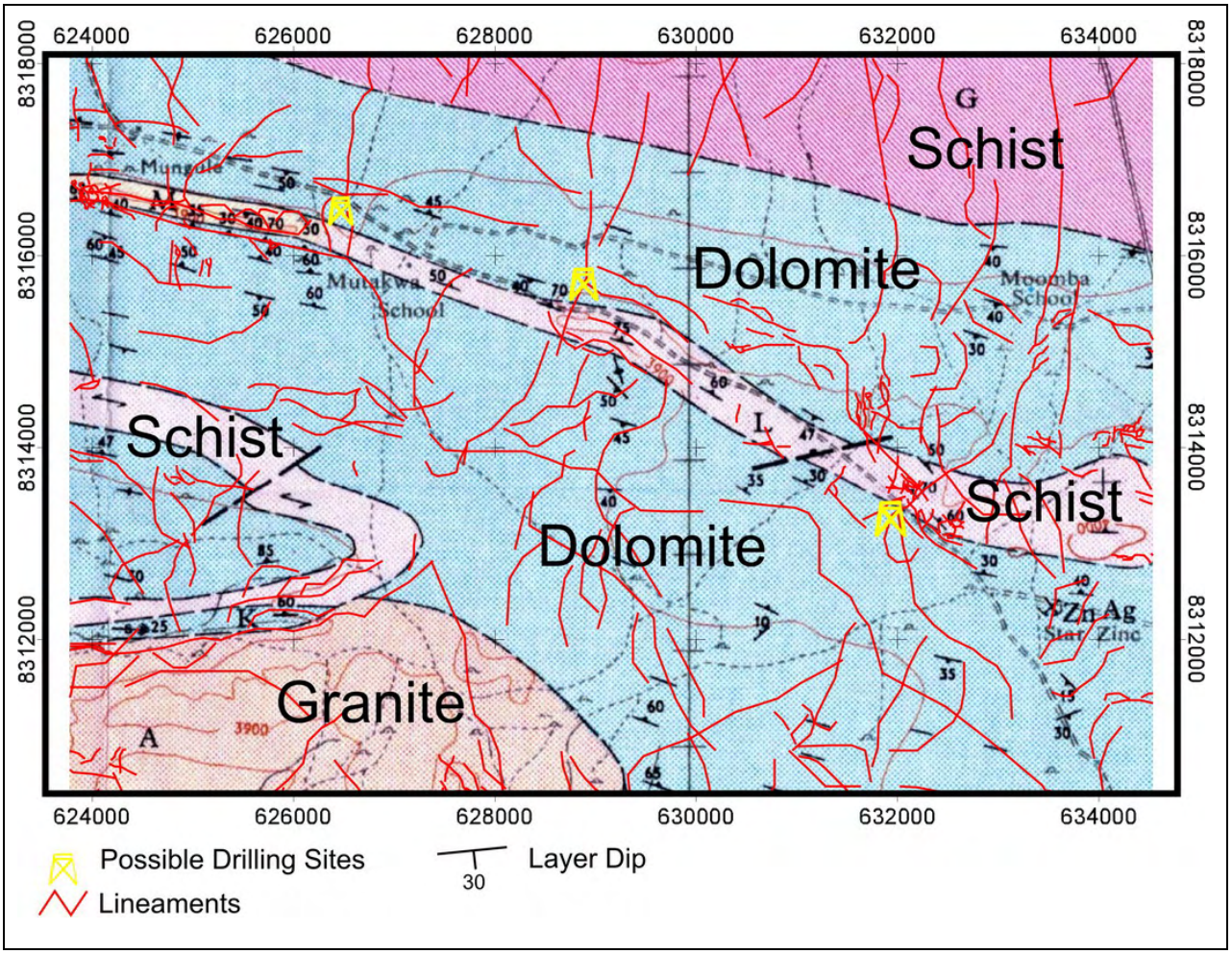

Figure 79: Examples of locations for possible drilling sites projected into modified geological map after Simpson et al. (1963).

Fault types

At a first consideration the transform fault type creating shear lenses appears to be “tighter” for water migration than the fault type of normal faulting depending on the different mechanisms of movement. The first type “smearing tight” the fault trace, the second type opening the fault trace by setting off the affected geological formation. On a closer view the fault-affected lithology type appears to take more control of permeability. For example the brittle schists affected by shear lenses are highly permeable for water in these zones. These observations could be subject for further investigations.

Drilling sites

The schists are almost impermeable for water migration except in zones of faults and joints where water migration appears to be even excellent. In those zones many boreholes operated by hand pumps are present.

The groundwater table is generally shallow in calcareous formations in the vicinity of schist ridges. This is true for locations where stratigraphical layers of calcareous formations are dipping towards the schist ridges channelling the water migration towards the ridges which appear to dam up groundwater. The likelihood of successful water drilling should increase at locations where additionally intersections of faults or joints are present (figure 79). Within the calcareous formations successful water drilling should be most likely in synclines and intersections of faults or joints.

9 References

BÄUMLE, R. & KANG'OMBA S. (2009): Development of a Groundwater Information & Management Program for the Lusaka Groundwater Systems. Desk study & proposed work program report, Technical cooperation Zambia / Germany: Ministry of Energy and Water Development and BGR, Lusaka.

GARRARD, P. (1968): The geology of the Chainama Hills area. – Report of the Geological Survey No. 24, Explanation of degree sheet 1528, NE quarter; Republic of Zambia, Ministry of Mines and Minerals Development, Geological Survey Department; 80 pages; Government Printer, Lusaka.

HANSON R. E., WILSON T. J. & H. MUNYANYIWA (1994): Geologic evolution of the Neoproterozoic Zambezi Orogenic Belt in Zambia. – J. of African Earth Sciences 18/2: 135-150, Elsevier Science Ltd.

NKHUWA D. C. W. (1996): Hydrogeological and engineering geological problems of urban development over karstified marble in Lusaka, Zambia. – Mitteilungen zur Ingenieur- und Hydrogeologie 63, 251 pages; Aachen.

PORADA, H. & BERHORST, V. (2000): Towards a new understanding of the Neoproterocoic-Early Palaeocoic Lufilian and northern Zambezi Belts in Zambia and the Democratic Republic of Congo. – J. of African Earth Sciences 30/3: 727-771, Elsevier Science Ltd.

SIMPSON J. G. (1962): The geology of the Mwembeshi River area.- Report of the Geological Survey No. 11, Explanation of degree sheet 1527, NE quarter, Northern Rhodesia Ministry of Labour and Mines; 29 pages; Government Printer, Lusaka.

SIMPSON J. G., DRYSDALL A. R. & H. H. J. LAMBERT (1963): The geology and groundwater resources of the Lusaka area.– Report of the Geological Survey No. 16, Explanation of degree sheet 1528, NW. quarter; Northern Rhodesia Ministry of Labour and Mines; 59 pages; Government Printer, Lusaka.

Appendix

Waypoints of measurements and field photos as mentioned in figures. Date of coordinates (decimal degrees and UTM) is WGS84.

Way-point no.	x, lat	y, long	x, UTM35L	y, UTM35L	Height asl [m]	date [ddmmyyy hh:mm]
1	-15.396599	28.245605	633670.94	8297421.82	1280.60	08.06.2009 12:51
2	-15.396704	28.245090	633615.60	8297410.52	1278.20	08.06.2009 12:59
3	-15.400212	28.245893	633699.54	8297021.93	1280.60	08.06.2009 13:21
4	-15.400161	28.246001	633711.16	8297027.50	1277.50	08.06.2009 13:34
5	-15.401362	28.246036	633714.15	8296894.61	1279.40	08.06.2009 14:18
6	-15.402914	28.244828	633583.51	8296723.66	1278.20	08.06.2009 14:36
7	-15.412741	28.238892	632940.18	8295640.16	1275.10	08.06.2009 14:59
8	-15.417370	28.206456	629456.30	8295147.80	1267.10	08.06.2009 15:22
9	-15.444408	28.274081	636695.96	8292114.76	1283.00	09.06.2009 09:40
10	-15.444804	28.274319	636721.24	8292070.79	1282.80	09.06.2009 09:54
11	-15.444873	28.274365	636726.13	8292063.13	1281.60	09.06.2009 10:00
12	-15.441239	28.276145	636919.52	8292464.04	1284.20	09.06.2009 10:17
13	-15.435852	28.286809	638067.41	8293053.20	1282.50	09.06.2009 11:17
14	-15.436602	28.286754	638061.01	8292970.26	1274.60	09.06.2009 11:25
15	-15.437353	28.286816	638067.17	8292887.14	1276.70	09.06.2009 11:36
16	-15.437612	28.287043	638091.35	8292858.34	1282.00	09.06.2009 11:45
17	-15.445049	28.305853	640104.85	8292023.39	1290.40	09.06.2009 12:31
18	-15.449737	28.305639	640078.74	8291504.88	1294.50	09.06.2009 12:45
19	-15.457800	28.306073	640119.89	8290612.56	1290.70	09.06.2009 13:09
20	-15.457766	28.306107	640123.56	8290616.30	1290.40	09.06.2009 13:11
21	-15.457598	28.306188	640132.36	8290634.83	1284.70	09.06.2009 13:15
22	-15.477420	28.309779	640504.31	8288439.50	1295.70	09.06.2009 13:45
23	-15.455310	28.320219	641639.44	8290878.77	1292.60	09.06.2009 14:21
24	-15.409109	28.334446	643197.70	8295980.77	1268.80	09.06.2009 14:51
25	-15.397462	28.338745	643667.10	8297266.47	1263.50	09.06.2009 15:25
27	-15.212162	27.950324	602069.56	8317985.60	1027.30	10.06.2009 12:40
28	-15.214693	27.953288	602386.71	8317704.24	1039.80	10.06.2009 14:21
29	-15.474127	28.331103	642794.41	8288789.75	1297.20	11.06.2009 10:28
30	-15.497098	28.332230	642899.55	8286247.60	1303.20	11.06.2009 11:29
31	-15.496826	28.331189	642788.06	8286278.39	1298.40	11.06.2009 11:59
32	-15.497121	28.331124	642780.88	8286245.79	1302.70	11.06.2009 12:12
33	-15.515772	28.338241	643531.51	8284177.58	1309.40	11.06.2009 13:07
34	-15.533110	28.343206	644052.07	8282256.04	1311.10	11.06.2009 13:43
35	-15.548972	28.366884	646580.61	8280485.03	1311.40	11.06.2009 14:44
36	-15.420759	28.179581	626570.12	8294788.85	1231.30	14.06.2009 18:33
37	-15.489646	28.444567	654956.87	8286994.04	1291.90	15.06.2009 09:26
38	-15.570241	28.467824	657390.91	8278059.99	1303.20	15.06.2009 11:05
39	-15.572903	28.464801	657064.68	8277767.70	1290.00	15.06.2009 11:27
40	-15.572786	28.464568	657039.78	8277780.81	1289.00	15.06.2009 11:37
41	-15.572478	28.463536	656929.34	8277815.65	1287.10	15.06.2009 11:47
42	-15.572473	28.463266	656900.39	8277816.40	1286.80	15.06.2009 11:59
43	-15.572392	28.463598	656936.05	8277825.12	1288.00	15.06.2009 12:13
44	-15.572048	28.463982	656977.50	8277862.90	1288.80	15.06.2009 12:20
45	-15.617264	28.478457	658495.18	8272849.40	1285.60	15.06.2009 13:26
46	-15.617520	28.478184	658465.71	8272821.28	1282.80	15.06.2009 13:46
47	-15.620297	28.476743	658309.07	8272515.10	1271.70	15.06.2009 14:21

Way-point no.	x, lat	y, long	x, UTM35L	y, UTM35L	Height asl [m]	date [ddmmyyy hh:mm]
48	-15.618013	28.478162	658462.98	8272766.75	1278.40	15.06.2009 14:32
49	-15.636835	28.502209	661026.67	8270666.16	1265.90	15.06.2009 15:03
50	-15.525462	28.472883	657967.62	8283010.67	1327.70	16.06.2009 10:17
51	-15.525361	28.473271	658009.32	8283021.55	1328.20	16.06.2009 10:20
52	-15.526703	28.478164	658533.18	8282869.45	1331.50	16.06.2009 10:38
53	-15.526976	28.478081	658524.06	8282839.31	1333.70	16.06.2009 10:43
54	-15.525470	28.473088	657989.61	8283009.63	1325.80	16.06.2009 11:06
55	-15.525337	28.471768	657848.11	8283025.32	1323.40	16.06.2009 11:20
56	-15.527520	28.414720	651726.99	8282825.06	1327.20	16.06.2009 12:09
57	-15.528388	28.414533	651706.29	8282729.16	1328.20	16.06.2009 12:14
58	-15.537321	28.396215	649734.93	8281753.74	1320.00	16.06.2009 12:53
59	-15.538003	28.396808	649798.04	8281677.87	1319.00	16.06.2009 13:02
60	-15.538351	28.397261	649846.38	8281639.05	1319.80	16.06.2009 13:06
61	-15.538554	28.397388	649859.85	8281616.50	1323.10	16.06.2009 13:21
62	-15.546075	28.367255	646622.45	8280805.29	1309.20	16.06.2009 13:57
63	-15.440380	28.314053	640987.92	8292534.59	1286.10	16.06.2009 15:44
64	-15.270064	28.266483	635993.59	8311407.48	1195.50	17.06.2009 10:57
65	-15.270724	28.266605	636006.27	8311334.39	1195.50	17.06.2009 11:02
66	-15.254132	28.232800	632386.24	8313190.80	1201.30	17.06.2009 11:54
67	-15.251848	28.231831	632283.60	8313444.07	1206.60	17.06.2009 12:21
68	-15.253914	28.229331	632013.80	8313217.03	1195.00	17.06.2009 12:40
69	-15.252288	28.230911	632184.51	8313395.95	1203.00	17.06.2009 13:08
71	-15.218048	28.154915	624042.57	8317228.51	1143.10	17.06.2009 14:11
72	-15.218212	28.154533	624001.44	8317210.58	1142.90	17.06.2009 14:21
73	-15.222246	28.151466	623669.64	8316766.06	1156.60	17.06.2009 15:07
74	-15.223082	28.151768	623701.59	8316673.40	1168.40	17.06.2009 15:15
75	-15.223401	28.151839	623709.03	8316638.07	1178.90	17.06.2009 15:20
76	-15.223479	28.151922	623717.90	8316629.40	1181.10	17.06.2009 15:31
77	-15.223793	28.152000	623726.09	8316594.61	1186.40	17.06.2009 15:35
78	-15.223470	28.174369	626129.03	8316617.54	1150.60	17.06.2009 16:18
79	-15.267284	28.199774	628831.21	8311755.64	1184.50	18.06.2009 10:23
80	-15.266709	28.200184	628875.60	8311819.01	1184.00	18.06.2009 10:38
81	-15.294229	28.197009	628517.86	8308776.40	1189.00	18.06.2009 11:22
82	-15.293320	28.194558	628255.22	8308878.41	1201.30	18.06.2009 11:37
83	-15.280559	28.189225	627690.29	8310293.28	1234.00	18.06.2009 12:45
84	-15.268020	28.185024	627246.72	8311682.90	1195.00	18.06.2009 13:55
85	-15.254403	28.179259	626635.77	8313192.67	1173.60	18.06.2009 14:25
86	-15.252351	28.174821	626160.36	8313422.26	1180.10	18.06.2009 14:27
87	-15.226305	28.139126	622341.80	8316323.98	1156.60	18.06.2009 14:49
88	-15.244215	28.219460	630959.66	8314295.98	1192.60	19.06.2009 10:09
89	-15.220957	28.173930	626083.37	8316895.80	1155.90	19.06.2009 10:33
90	-15.219736	28.145904	623073.65	8317046.87	1141.70	19.06.2009 11:19
91	-15.219748	28.146122	623097.06	8317045.42	1141.90	19.06.2009 11:27
92	-15.219907	28.146184	623103.63	8317027.80	1141.70	19.06.2009 11:28
93	-15.232153	28.134685	621861.42	8315679.53	1159.70	19.06.2009 11:46
94	-15.246285	28.138863	622302.00	8314113.83	1163.60	19.06.2009 12:02
95	-15.250830	28.138746	622286.81	8313611.10	1158.30	19.06.2009 12:19
96	-15.251325	28.133731	621747.91	8313559.15	1157.30	19.06.2009 12:32
97	-15.250025	28.123820	620684.23	8313708.48	1158.30	19.06.2009 12:45
98	-15.243547	28.112136	619433.03	8314431.55	1152.70	19.06.2009 12:57
99	-15.241511	28.108384	619031.20	8314658.84	1156.30	19.06.2009 13:16
100	-15.241390	28.102519	618401.35	8314675.42	1147.20	19.06.2009 13:54

Way-point no.	x, lat	y, long	x, UTM35L	y, UTM35L	Height asl [m]	date [ddmmyyy hh:mm]
101	-15.237146	28.097121	617823.95	8315147.83	1150.30	19.06.2009 14:20
102	-15.236332	28.095473	617647.40	8315238.77	1149.90	19.06.2009 14:28
103	-15.227979	28.096227	617733.03	8316162.41	1149.10	19.06.2009 14:37
104	-15.223292	28.095860	617696.22	8316681.10	1145.50	19.06.2009 14:44
105	-15.221682	28.096660	617783.04	8316858.78	1142.40	19.06.2009 14:55
106	-15.211966	28.098906	618029.70	8317932.39	1124.10	19.06.2009 15:03
107	-15.398749	28.307061	640265.56	8297144.94	1244.50	21.06.2009 17:12
108	-15.496573	28.336528	643361.00	8286302.82	1295.00	22.06.2009 12:50
109	-15.495990	28.336271	643333.83	8286367.49	1290.40	22.06.2009 13:04
110	-15.498315	28.339698	643699.88	8286107.97	1298.60	22.06.2009 13:15
111	-15.475371	28.341988	643961.43	8288644.85	1296.20	22.06.2009 13:43
112	-15.394248	28.275345	636864.45	8297663.26	1247.20	23.06.2009 09:53
113	-15.213789	28.058175	613653.51	8317752.33	1116.70	23.06.2009 11:22
114	-15.213951	28.058132	613648.80	8317734.44	1116.20	23.06.2009 11:39
115	-15.236141	28.051635	612939.09	8315283.09		23.06.2009 11:55
116	-15.251459	28.049754	612728.90	8313589.54	1118.90	23.06.2009 12:19
117	-15.251869	28.050146	612770.78	8313543.98	1140.00	23.06.2009 12:29
118	-15.251534	28.050237	612780.73	8313580.99	1139.30	23.06.2009 12:37
119	-15.266726	28.011258	608586.74	8311920.24	1062.10	23.06.2009 14:32
120	-15.256219	28.290264	638556.62	8312924.16	1204.20	24.06.2009 10:27
121	-15.253133	28.292425	638790.74	8313264.19	1187.80	24.06.2009 10:38
122	-15.249388	28.294863	639055.06	8313676.95	1187.60	24.06.2009 10:56
123	-15.259166	28.293359	638887.09	8312596.16	1225.60	24.06.2009 11:20
124	-15.259557	28.293829	638937.32	8312552.60	1236.40	24.06.2009 11:33
125	-15.259617	28.294477	639006.87	8312545.55	1233.00	24.06.2009 11:44
126	-15.259594	28.294888	639051.03	8312547.83	1241.20	24.06.2009 11:56
127	-15.269795	28.272151	636602.48	8311433.69		24.06.2009 12:44
128	-15.245218	28.256888	634979.02	8314162.17	1176.00	24.06.2009 12:54
129	-15.244116	28.242659	633451.43	8314292.85	1174.60	24.06.2009 13:13
130	-15.248931	28.228328	631909.19	8313768.90	1191.20	24.06.2009 13:26
131	-15.199440	28.031552	610801.28	8319353.34	1081.60	24.06.2009 14:18
132	-15.350117	28.502671	661298.50	8302388.91	1124.10	25.06.2009 13:53
133	-15.809274	28.361066	645771.68	8251689.72	1160.90	26.06.2009 10:45
134	-15.803926	28.359894	645649.96	8252282.23	1130.90	26.06.2009 11:27
135	-15.798272	28.356644	645305.85	8252910.03	1085.20	26.06.2009 11:48